Robust Network-Constrained Energy Management of a Multiple Energy Distribution Company in the presence of Multi-Energy Conversion and Storage Technologies

Mirzaei, Mohammad Amin ; Zare, Kazem; Mohammadi-Ivatloo, Behnam ; Marzband, Mousa; Anvari-Moghaddam, Amjad

Published in:
Sustainable Cities and Society

DOI (link to publication from Publisher):
10.1016/j.scs.2021.103147

Publication date:
2021

Document Version
Accepted author manuscript, peer reviewed version

Robust Network-Constrained Energy Management of a Multiple Energy Distribution Company in the presence of Multi-Energy Conversion and Storage Technologies

Abstract

Multi-energy systems have been developed to supply the multi-energy users economically by considering the physical limitations of different energy networks. This paper proposes a new entity called multiple energy distribution company (MEDC) to meet the electricity, gas, and heat demands of consumers in the presence of renewable energy resources (RESs) and multi-energy conversion technologies with the lowest operating cost. To achieve a more accurate scheduling model, a multi-energy flow model is used that involves practical constraints of the power distribution network, heating distribution network (HDN) and natural gas distribution network simultaneously. A variable mass flow and temperature control strategy is applied in the HDN to make a high-performance energy supply scheme. Multi-energy storage systems (MESSs) and integrated demand response (IDR) are also considered to increase the flexibility of the MEDC for serving multi-type energy demands. Moreover, a hybrid robust-stochastic optimization technique is adopted to handle the system uncertainties, where the uncertainties related to RESs and energy prices are addressed under a scenario-based stochastic programming and a robust optimization technique, respectively. The simulation results demonstrate that the efficient use of MESSs and IDR improves the performance of multi-energy generation units in the presence of multi-energy distribution network constraints and reduces the total operation cost by 15%.

Keywords- Multi-energy systems, heat distribution network, gas distribution network, robust optimization, multi-energy storage systems, integrated demand response, hybrid optimization approach

Nomenclature

Indexes and sets

t	Scheduling intervals
s	Scenarios
g	Gas suppliers
i	GF-CHP and NGFPG units
w	Wind power units
v	PV units
e	EB units
b, b', b''	PDN buses
k, f	GDN nodes
h	HDN nodes
el	Electric demand
gl	Residential gas demand
hl	Heat demand
es	ESS
gs	GSS
hs	HSS
NT	Number of scheduling intervals
NEL	Number of electric demands
NGL	Number of gas demands
NHL	Number of heat demands
NP	Number of CHP and NGFPG units
NC	Number of NGFPF units
$NCHP$	Number of CHP units
NES	Number of ESSs
NGS	Number of GSSs
NHS	Number of HSSs
NW	Number of wind power units
NV	Number of PV units
NEB	Number of EB units
AS^- / AR^-	Set of supply/return pipes ending at nodes
AS^+ / AR^+	Set of supply/return pipes starting at nodes

Parameters

$P_i^{\min}, P_i^{\max}$	Min/Max power limit of generation units
$PD_{es}^{\min}, PD_{es}^{\max}$	Min/Max discharge rate of ESSs
$PC_{es}^{\min}, PC_{es}^{\max}$	Min/Max charge rate of ESSs
$ES_{es}^{\min}, ES_{es}^{\max}$	Min/Max capacity of ESSs
$HD_{hs}^{\max}, GD_{gs}^{\max}$	The maximum discharge rate of HSSs/GSSs
$HC_{hs}^{\max}, GC_{gs}^{\max}$	The maximum charge rate of HSSs/GSSs
$HS_{hs}^{\min}, HS_{hs}^{\max}$	Min/Max capacity of HSSs
$GS_{gs}^{\min}, GS_{gs}^{\max}$	Min/Max capacity of GSSs
$EB_e^{\max}$	Maximum power consumption of EBs
$\eta_{es}^{es\_dis}, \eta_{es}^{es\_ch}$	Discharge/Charge efficiency of ESSs
$\eta_{hs}^{hs\_dis}, \eta_{hs}^{hs\_ch}$	Discharge/Charge efficiency of HSSs
$\eta_{hs}^{hs\_dis}, \eta_{hs}^{hs\_ch}$	Discharge/Charge efficiency of GSSs
$MOT_i, MOFT_i$	Minimum on/off time of power units
RU_i , RD_i	Up/Down ramp rate of power units
$RU_g^{\sup}$, $RD_g^{\sup}$	Up/Down ramp rate of gas suppliers
$x_{b,b'}, r_{b,b'}$	Reactance/Resistance of PDN lines
$C_{el}^{edr}, C_{hl}^{hdr}, C_{gl}^{gdr}$	The implementation cost of IDR
$EL_{el}^{edr}, EL_{hl}^{hdr}, EL_{gl}^{gdr}$	Electric/Heat/ Gas demands
$\chi_{el}^{E}, \chi_{hl}^{H}, \chi_{gl}^{G}$	Maximum shiftable electric/heat/gas demand
$P_{w,t,s}^{f\_wind}$, $P_{v,t,s}^{f\_pv}$	Forecasted power of wind/PV
$v_b^{\max}, v_b^{\min}$	Max/Min voltage in the PDN
$T_h^{su,\max}, T_h^{su,\min}$	Max/Min supply pipelines temperature
$T_h^{re,\max}, T_h^{re,\min}$	Max/Min return pipelines temperature
$\upsilon_k^{\max}$, $\upsilon_k^{\min}$	Max/Min pressure of the GDN
HR_i	Heat rate of power generation units
COP_e	Coefficient of performance of EB units
$i_{b,b'}^{\max}$	The maximum current of PDN lines
$\lambda_t^{e\_mt}$, $\lambda_t^{g\_mt}$	Power/Gas market price
λ^{coal}	Coal fuel price

Variables

$P_{i,t,s}, Q_{i,t,s}$	Active/Reactive power generated by GF-CHP and NGFPG units
$P_{t,s}^{mt}, G_{t,s}^{mt}$	The energy exchanged with power/gas markets
$B_{i,t,s}$	Commitment status of power generation units
$Y_{i,t,s}$	Start-up state of power generation units
$X_{i,t,s}$	Shut-down state of power generation units
$BD_{es,t,s}^{-}, BC_{es,t,s}$	Discharge/charge status of ESSs
$STC_{i,t,s}, SHC_{i,t,s}$	Start-up/shut-down cost of power units
$H_{i,t}, H_{e,t,s}^{EB}$	The heat generated by GF-CHP/EB units
$ELR_{el,t,s}^{up}, ELR_{el,t,s}^{dn}$	Increased/decreased electric demand
$HLR_{hl,t,s}^{up}, HLR_{hl,t,s}^{dn}$	Increased/decreased heat demand
$GLR_{gl,t,s}^{up}, GLR_{gl,t,s}^{dn}$	Increased/decreased gas demand
$P_{w,t,s}^{wind}, Q_{w,t,s}^{wind}$	Active/Reactive power output of wind
$P_{v,t,s}^{pv}, Q_{v,t,s}^{pv}$	Active/Reactive power output of PV
$PD_{es,t,s}, PC_{es,t,s}$	Discharge/Charge rate of ESSs
$HD_{hs,t,s}, HC_{hs,t,s}$	Discharge/Charge rate of HSSs
$GD_{gs,t,s}, GC_{gs,t,s}$	Discharge/Charge rate of GSSs
$ES_{es,t,s}, HS_{hs,t,s}, GS_{gs,t,s}$	Available power/heat/gas level of in ESSs/GSSs/HSSs
$EL_{el,t,s}^{dr}, HL_{hl,t,s}^{dr}, GL_{gl,t,s}^{dr}$	Power/Heat/Gas demand after the IDR
$PF_{b,b',t,s}, QF_{b,b',t,s}$	Active/Reactive power of PDN lines
$i_{b,b',t,s}$	The current of the PDN lines
$v_{b,t,s}$	The voltage of the PDN buses
$M_{i,t,s}, M_{e,t,s}^{EB}$	The mass flow rate of GF-CHP/EB units
$MC_{hs,t,s}, MD_{hs,t,s}$	The mass flow rate of charge/discharge of HSS
$M_{hl,t,s}^{HL}$	The mass flow rate of heat demand
$M_{j,t,s}^{su}, M_{j,t,s}^{re}$	The mass flow rate of supply/return pipelines
$T_{h,t,s}^{su}, T_{h,t,s}^{re}$	Supply/Return pipelines water temperature
$\upsilon_{k,t,s}$	The pressure of the GDN nodes
$F_{k,f,t,s}$	The gas flow of the GDN lines
$G_{g,t,s}^{sup}$	Gas supplied by gas suppliers
$\sigma_s, \psi_{t,s}$	Dual variables

$U_{t,s}$ Auxiliary variable

1. Introduction

1.1. Motivation

Energy distribution systems are generally considered as individual networks with separate energy vectors such as power, gas, and heat [1]. Energy distribution companies are responsible for meeting the energy demand of end-users at the lowest cost [2, 3]. A heat distribution network (HDN) is one of the energy carrier networks that has received much attention in recent years in many Nordic countries, such as Denmark. HDN is a promising tool for saving energy and reducing carbon emissions [4]. In HDN, heat is mainly generated by gas-fired based combined heat and power (GF-CHP) units and electric boilers (EBs) at big centralized stations and transmitted to the heat customers via the underground pipelines as hot water or steam instead of fuel [5, 6]. As such, buildings do not require independent heating units, which means that there is no need to transfer gas or oil to the buildings. With the increasing use of highly efficient energy conversion technologies, such as GF-CHP units and EBs, the independent structure of traditional energy distribution companies must be shifted towards integrated energy management to make the best use of multi-energy conversion and storage technologies and meet the multi-energy demands at the lowest cost [7, 8]. To this end, a new entity called multiple energy distribution company (MEDC) is introduced to supply the power, gas and heat demands simultaneously, where the physical constraints of the multi-energy distribution network are considered to achieve a high-performance scheduling model.

1.2. Literature review

Optimal scheduling of energy service providers to meet the various demands of consumers under integrated management in the presence of energy conversion facilities has attracted the attention of researchers in recent years. In [9], the authors proposed a hybrid info-gap/interval/stochastic approach to calculate optimal scheduling of energy hubs integrated into power distribution networks (PDNs) by considering wind power, demand, and energy price uncertainties. In [10], a hybrid robust/stochastic approach is proposed to determine the optimal participation of a multi-energy service provider in multi-energy markets, where the role of energy conversion technologies has been investigated on the profit

of multi-energy service provider. In [11], a scenario-based two-stage iterative technique is adopted for optimal scheduling of power and thermal-based energy storage systems in multi-energy networks. In [12], the stochastic optimal scheduling of a coupled power, heat and gas delivery system is studied by the full consideration of carbon-capture-based power-to-gas technology, renewable energy resources and GF-CHP units. In [13], a conditional-value-at-risk based stochastic model is presented for managing the uncertainties of multi-energy demands and wind power in a multi-energy system, where the P2G technology and compressed air energy storage has been introduced as flexible options to minimize the total operation cost.

Some of the literature focused on the interaction between power and heat distribution networks through modelling the physical constraints of both systems in recent years. In [14], the interconnection between PDN and HDN is considered through CHP units and EBs, where the DHN operator solves a heat flow problem according to the nodal electricity prices determined from the power flow problem and obtains the best heat generation strategy. A new integrated power and heat scheduling model is formulated in [15] that includes the thermal inertia of the HDN to increase the flexibility of CHP units for integrating wind power. A robust optimization approach for coordinated electrical and heat distribution networks is proposed in [16], where smart buildings have been modelled as equivalent storage devices to improve operational flexibility and provide extra reserves in PDNs. In [17], the optimum unit commitment is determined in interlinked PDN and HDN under a two-stage robust optimization technique with variable wind power output. A high-efficient model is also proposed in [18] to injection heat to HDN while generating hydrogen, where power-to hydrogen-to heat technology has been considered for the power-heat-hydrogen dispatch in linked PDN and DHN. In [19], a comprehensive technical evaluation of the operation of coupled PDN and HDN is studied, where EBs have been introduced to support the transition to intelligent energy systems.

Several works of literature also evaluated interdependency between power and gas distribution networks through modelling the physical constraints of both systems. A dynamic pricing problem in power and gas distribution networks is provided in [20], where power and gas companies act as leaders in the upper level and obtain their optimal dynamic prices via modelling the demand response presented by integrated aggregators in the lower level. A two-step data-driven DRO is proposed in [21] to model

the optimization problem of combined PDN and gas distribution network (GDN), in which the minimum voltage deviation and minimum operation cost are determined through active power management and reactive power provision in both day-ahead and real-time step. In [22], authors studied a decentralized structure for the optimal scheduling of integrated PDN and GDN in networked energy hubs, where the integrated system operator specifies the optimal dispatch of units while maintaining the privacy of stockholders' data. In [23], a tri-level robust optimization method is introduced to improve the power and gas-based distribution networks resilience with respect to the worst N-k contingencies. The authors studied a coordinated scheduling approach for the power and gas integrated distribution network in [24], considering combined cooling, heating and power units, where the integrated system operator is responsible for serving power, heat and cooling demands. An integrated scheduling model for PDN and GDN is presented in [25], which considers technical and environmental constraints in the presence of power and gas-based storage systems. In [26], a two-stage stochastic model for the optimal operation of combined PDN and GDN is presented, which integrates multiple energy systems such as power, heat, and gas. A column-and-constraint generation method is solved in [27] for optimal operation of the power distribution network, where the bidirectional physical and economic interactions with the gas system are considered.

1.3. Gaps and contributions

It can be realized from the investigated literature that the optimal scheduling of a network-constrained multi-energy distribution system with multi-energy storages and integrated demand response (IDR) have not been appropriately investigated. The significant gaps in the studied literature can be defined as follows:

1) In [9-13], researchers have not considered the physical constraints of gas and heat distribution networks in the optimal operation of multi-energy systems and have only evaluated the role of emerging energy resources in such systems.
2) Some of the literature, such as [14-27], mainly focused on the cooperation of PDN and HDN or PDN and GDN and did not consider the interaction of all three distribution networks simultaneously. Since the interdependence of energy networks increases with the rise of GF-CHP units, it is necessary to consider a network-constrained integrated energy management structure.

3) In [14-20], the authors mainly modelled the HDN based on constant mass flow and variable temperature (CF-VT) control strategy, which has less flexibility compared with variable mass flow and variable temperature (VF-VT) control strategy.
4) The effect of IDR in network-constrained multi-energy distribution systems has not been investigated in [14-27].

Based on the gaps defined above and Table 1, the main contributions of this paper can be described in detail as follows:

- A new entity called multiple energy distribution company (MEDC) is proposed, in which the MEDC operator meets the electricity, gas and heating demand of the consumers simultaneously at the lowest cost, while the physical constraints related to the power, gas and heating distribution networks and their interaction with each other are fully taken into account.
- A variable mass flow and variables temperature (VF-VT) control strategy is proposed to increase the flexibility of HDN.
- A coordinated scheduling model for multi-energy storage systems and IDR is considered to enhance the flexibility of the MEDC for serving multi-type energy demands.
- A hybrid robust-stochastic optimization approach is adopted to manage the uncertainties of the multi-energy distribution network. In the proposed model, uncertainties associated with wind power and photovoltaic units are handled by a risk-neutral stochastic approach, and a risk-averse approach is suggested to consider the fluctuations of market price without the need for probability distribution function (PDF). The proposed hybrid technique enables the operator to use both risk-neutral and risk-averse strategies simultaneously with respect to the nature of uncertainties to adopt a more efficient decision-making model.

1.4. Paper organization

The rest of this paper is organized as follows: Section 2 is related to the description of the proposed MEDC. Section 3 presents the problem formulation that includes objective function with corresponding constraints. Section 4 consists of numerical and simulation results. Finally, section 5 concludes the paper.

Table 1: Comparison between the proposed model and reviewed literature

Refs	Modelling energy distribution networks			IDR	Multi-energy storage			Control strategy of HDN		Uncertainty modelling approach
	PDN	GDN	HDN		EES	GSS	HSS	CF-VT	VF-VT	
[9]	✓	-	-	✓	✓	-	✓	-	-	Hybrid IGDT-stochastic-interval
[13]	-	-	-	-	✓	✓	✓	-	-	CVaR-based stochastic
[16]	✓	-	✓	-	✓	-	✓	✓	-	Distributionaly robust optimization
[17]	✓	-	✓	-	✓	-	✓	✓	-	Two-stage distributionaly robust optimization
[21]	✓	✓	-	-	✓	✓	-	-	-	Robust optimization
[23]	✓	✓	-	-	-	✓	-	-	-	Robust optimization
[24]	✓	✓	-	-	✓	-	✓	-	-	-
[25]	✓	✓	-	-	✓	✓	-	-	-	-
Proposed model	✓	✓	✓	✓	✓	✓	✓	-	✓	Hybrid robust-stochastic optimization

2. Problem description

The MEDC operator acts as an intermediate link between the multi-energy markets and multi-energy users (MEUs). The MEDC operator predicts energy prices and MEUs' demand based on historical data. Accordingly, the MEDC operator solves a self-scheduling problem according to the forecasted energy prices and demand data to specify the selling/buying strategy with the energy markets by considering multi-energy distribution network constraints. Figure 1 represents the structure of the proposed MEDC. The MEDC operator can purchase power and gas from the multi-energy market or use energy resources under his ownership to satisfy MEUs' demand. Also, it can sell the excess power to the market to reduce the total operation cost. The proposed MEDC includes a GF-CHP unit, non-gas-fired power generation (NGFPG) unit, EB unit, gas suppliers, electrical storage system (ESS), gas storage system (GSS), heat storage system (HSS), wind power and PV units to satisfy the demand of MEUs.

Furthermore, the MEDC operator can use the flexibility of MEUs under IDR programs and apply such programs based on incentives/ rewards paid to the responsive loads. According to the IDR concept [28-30], the operator can shift the heat demand along with power demand in peak power price hours to the cheaper price hours, thus reducing the EBs' power consumption and the electricity purchase from the power market in peak hours. In addition, during the hours when gas demand is high, due to the higher priority of residential and commercial gas demand, the gas fuel required by gas-fired units may not be supplied during such hours. Therefore, by shifting part of the flexible gas demand to other hours, the pipeline congestion issue in the GDN is reduced, which in turn increases the gas-fired unit's participation such as GF-CHP units and reduces the operation cost of MEDC. So, applying these technologies can provide suitable opportunities for the MEDC operator to meet its responsibilities at

the lowest operation cost. In addition, the stochastic nature of renewable energy resources (RESs) such as wind energy and PV units and the uncertainty of electricity prices pose a challenge for the MEDC operator to achieve integrated optimal management using GF-CHP units, EBs and other facilities. To this end, a hybrid robust-stochastic technique is adopted in this paper to manage the uncertainties related to wind power and PV units and power price. Accordingly, a risk-neutral stochastic approach is used to handle RESs uncertainty, and the robust optimization technique is considered to manage power price fluctuations since it has more severe uncertainty compared to RESs.

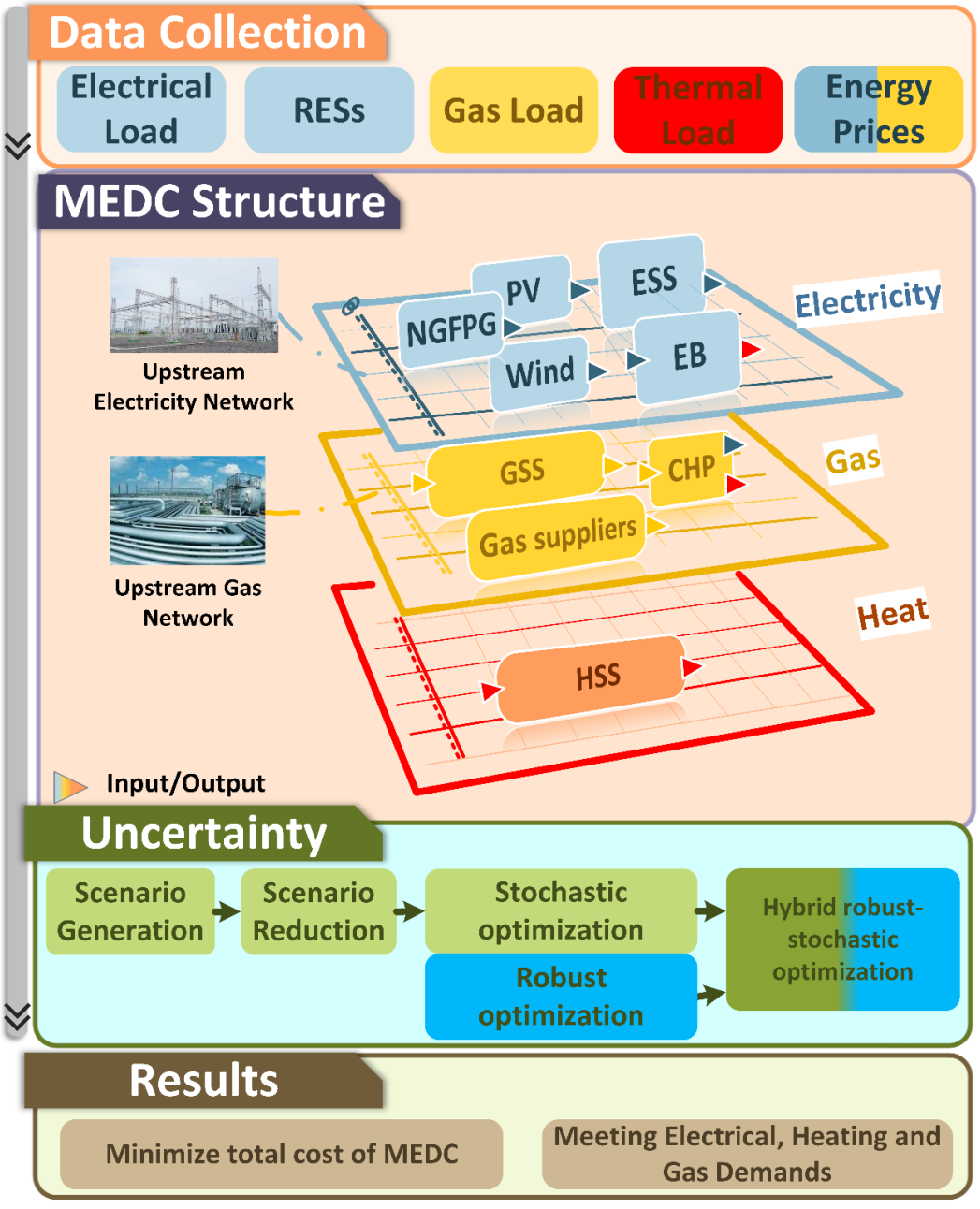

Fig. 1. Structure of the proposed MEDC

3. Problem formulation

To manage the uncertainties in the multi-energy distribution network, the optimal energy management problem of the proposed MEDC is formulated under a pure stochastic approach and hybrid robust-stochastic optimization technique, respectively.

3.1. Integrated energy management under stochastic approach

A risk-neutral stochastic scheduling framework for the proposed MEDC is described in this section. Stochastic programming is a suitable way to make decisions in probabilistic and unknown conditions [31]. The MEDC operator uses the stochastic programming to obtain the optimal generation scheme of GF-CHP and NGFPG units, EBs, amount of energy sold/purchased to/from the multi-energy market, as well as the discharge and charge scheme of the energy storages and optimal implementation of IDR programs. The uncertainties relevant to wind power and PV units are expressed via various scenarios based on historical or forecasted data [32]. In addition, a practical scenario reduction approach is also applied to decrease the scenarios number and the computational difficulty of the optimization problem. The Monte Carlo simulation method is used to create a set of possible scenarios for modelling the uncertainties in the proposed multi-energy distribution network.

Wind power uncertainty modelling: Many methods such as the time-series approach and the clustering method are considered to model the uncertain behaviour of wind power generation. However, Weibull PDF has been widely applied to model the wind speed (v^{speed}) changes due to its extreme adaptability. Weibull PDF is represented in (1), where k and c are the shape and scale factors, respectively [33, 34]. After generating scenarios using Weibull distribution, wind power production that depends on wind speed can be calculated as (2).

$$PDF(v^{speed}) = (\frac{k}{c})(\frac{v^{speed}}{c})^{k-1} \exp\left[-(\frac{v^{speed}}{c})^{k}\right] \tag{1}$$

$$P_{w,t,s}^{wind} = \begin{cases} 0 & v_{w,t,s}^{speed} < v_w^{in}, v_{w,t,s}^{speed} \geq v_w^{out} \\ (\frac{v_{w,t,s}^{speed} - v_w^{in}}{v_w^{r} - v_w^{in}}) P_w^{wind,\max} & v_w^{in} \leq v_{w,t,s}^{speed} < v_w^{r} \\ P_w^{wind,\max} & v_w^{r} \leq v_{w,t,s}^{speed} < v_w^{out} \end{cases} \tag{2}$$

Where $P_w^{wind,\max}$ is rated power of wind plant; v_w^{in}, v_w^{out} and v_w^{r} are defined as the cut-in, cut-out and rated wind speed, respectively.

- ***PV power uncertainty modelling:*** The power generated by a PV system is associated with three parameters: solar radiation, ambient temperature, and plate profile, where solar radiation (I^T) is an indeterminate parameter that is usually modelled by Beta PDF as described in (3) [33, 34]. The parameters of this distribution function are specified with α and β as shape parameters. After producing scenarios using Beta distribution, PV power production that depends on solar radiation can be provided as (4).

$$PDF(I^T) = \frac{\Gamma(\alpha+\beta)}{\Gamma(\alpha)+\Gamma(\beta)} * (I^T)^{\alpha-1} * (1-I^T)^{\beta-1} \tag{3}$$

$$P_{v,t,s}^{pv} = S_v^{pv} \eta_v^{pv} I_{v,t,s}^T \tag{4}$$

Where S_v^{pv} and η_v^{pv} are defined as the area and efficiency of the PV system, respectively.

- ***Scenario reduction:*** In this paper, the SCENRED toolbox in General Algebraic Modelling System (GAMS) software is applied for scenario reduction procedure that includes two reduction algorithms of the backward method and forward method. The fast-backwards reduction approach is adopted in this paper based on runtime and performance accuracy [13].

3.1.1 Objective function

The main purpose of the proposed model is to minimize the total operating cost of MEDC, as defined in (5). The objective function consists of eight terms. The first term establishes the power exchanged between the MEDC and the power market. The second term refers to the gas purchased from the gas market. The third term is related to the cost of gas suppliers managed by the MEDC operator. The fourth term is associated with the cost of NGFPG units that includes fuel cost and start-up and shut-down costs. The fifth term defines the maintenance cost of all power generation units. The three last terms also demonstrate the incentive cost of the IDR program.

$$\min \sum_{s=1}^{NS} p_s \left[\sum_{t=1}^{NT} \left[\begin{array}{l} \lambda_t^{e\_mt} P_{t,s}^{mt} + \lambda_t^{g\_mt} G_{t,s}^{mt} + \sum_{g=1}^{NG} C_g G_{g,t,s}^{\sup} + \sum_{i=1}^{NC} \left[\lambda^{coal} HR_i P_{i,t,s} + STC_{i,t,s} + SHC_{i,t,s} \right] \\ + \sum_{i=1}^{NP} MC_i P_{i,t,s} + \sum_{el=1}^{NEL} C_{el}^{edr} \left(ELR_{el,t,s}^{up} + ELR_{el,t,s}^{dn} \right) + \sum_{hl=1}^{NHL} C_{hl}^{hdr} \left(HLR_{hl,t,s}^{up} + HLR_{hl,t,s}^{dn} \right) \\ + \sum_{gl=1}^{NGL} C_{gl}^{gdr} \left(GLR_{gl,t,s}^{up} + GLR_{gl,t,s}^{dn} \right) \end{array} \right] \right] \tag{5}$$

3.1.2 PDN's constraints

Constraints related to GF-CHP and NGFPG units connected to the PDN are described as (6)-(15). Active and reactive power generation limits of units are expressed by (6)-(7). Constraints (8) and (9) determine the start-up and shut-down status of all units. Constraints (10) and (11) show the cost of start-up and shut-down of NGFPG units. Limitations of ramp-up and ramp-down rates of power generation units in consecutive time intervals are demonstrated by (12) and (13). Constraints related to minimum on-time and minimum off-time of power generation units are expressed by (14) and (15). The constraint of EBs connected to PDN is defined as (16), which indicates the power consumption limit of these units. Limit constraints for active and reactive power dispatch of wind power and PV units are defined by (17)-(18).

$$P_i^{\min} B_{i,t,s} \le P_{i,t,s} \le P_i^{\max} B_{i,t,s} \tag{6}$$

$$Q_i^{\min} B_{i,t,s} \le Q_{i,t,s} \le Q_i^{\max} B_{i,t,s} \tag{7}$$

$$Y_{i,t,s} - X_{i,t,s} = B_{i,t-1,s} - B_{i,t,s} \tag{8}$$

$$Y_{i,t,s} + X_{i,t,s} \le 1 \tag{9}$$

$$STU_{i,t,s} \ge C_i^{SU} Y_{i,t,s} \quad \forall i \in NC \tag{10}$$

$$STD_{i,t,s} \ge C_i^{SD} X_{i,t,s} \quad \forall i \in NC \tag{11}$$

$$P_{i,t,s} - P_{i,t-1,s} \le (1 - Y_{i,t,s}) RU_i + Y_{i.t,s} P_i^{\min} \tag{12}$$

$$P_{i,t-1,s} - P_{i,t,s} \le (1 - X_{i,t,s}) RD_i + X_{i.t,s} P_i^{\min} \tag{13}$$

$$\sum_{t'=t+2}^{t+MOT_i} (1 - B_{i,t',s}) + MOT_i (B_{i,t,s} - B_{i,t-1,s}) \le MOT_i \tag{14}$$

$$\sum_{t'=t+2}^{t+MOFT_i} B_{i,t',s} + MOFT_i (B_{i,t-1,s} - B_{i,t,s}) \le MOFT_i \tag{15}$$

$$0 \le EB_{e,t,s} \le EB_e^{\max} \tag{16}$$

$$\sqrt{(P_{w,t,s}^{wind})^2 + (Q_{w,t,s}^{wind})^2} \le P_w^{wind,\max} \tag{17}$$

$$\sqrt{(P_{v,t,s}^{pv})^2 + (Q_{v,t,s}^{pv})^2} \le P_v^{pv,\max} \tag{18}$$

Limitations related to the ESS connected to PDN are also described by (19)-(24). The ESS cannot be operated simultaneously in charge and discharge modes, as presented in (19). Constraints associated with charge and discharge power of ESS are defined by (20) and (21), respectively. State of Charge (SoC) of ESS in each hour is calculated as (22). The capacity limitation of ESS is also expressed by

(23). The initial and final SoC of ESS should be equal, as described in (24). Constraint (25) indicates that the electricity demand reduced in each hour should be shifted to other hours. Electricity demand after implementing IDR is expressed by (26). Shiftable active and reactive demands in each hour are limited, as shown by (27)-(28).

$$BC_{es,t,s} + BD_{es,t,s} \le 1 \tag{19}$$

$$PC_{es}^{\min} BC_{es,t,s} \le PC_{es,t,s} \le PC_{es}^{\max} BC_{es,t,s} \tag{20}$$

$$PD_{es}^{\min} BD_{es,t,s} \le PD_{es,t,s} \le PD_{es}^{\max} BD_{es,t,s} \tag{21}$$

$$ES_{es,t,s} = ES_{es,t\text{-}1,s} + \eta_{es}^{es\_ch} PC_{es,t,s} - \frac{PD_{es,t,s}}{\eta_{es}^{es\_dis}} \tag{22}$$

$$ES_{es}^{\min} \le ES_{es,t,s} \le ES_{es}^{\max} \tag{23}$$

$$ES_{es,t=0} = ES_{es,t=24,s} \tag{24}$$

$$\sum_{t=1}^{NT} (ELR_{el,t,s}^{up} - ELR_{el,t,s}^{dn}) = 0 \tag{25}$$

$$EL_{el,t,s}^{dr} = EL_{el,t}^{0} + ELR_{el,t,s}^{up} - ELR_{el,t,s}^{dn} \tag{26}$$

$$EL_{el,t}^{0}(1-\chi_{el}^{E}) \le EL_{el,t,s}^{dr} \le EL_{el,t}^{0}(1+\chi_{el}^{E}) \tag{27}$$

$$QL_{el,t,s}^{dr} = EL_{el,t,s}^{dr} \tan\phi \tag{28}$$

The active and reactive power balance in each bus is made by constraints (29) and (30), respectively. Constraint (31) represents the relation between the voltage magnitude, the current magnitude and power flow. The limit constraint for active and reactive power transferred from line *LE* and the upper and lower limit constraints for branch current and voltage magnitude are defined by (32)-(33), respectively.

$$\sum_{(b,b'')\in LE} PF_{b,b',t,s} = PF_{b,b'',t,s} - r_{b,b''}(i_{b,b'',t,s})^2 + P_{t,s}^{mt} + \sum_{i=1}^{NP_b} P_{i,t,s} + \sum_{w=1}^{NW_b} P_{w,t,s}^{wind} + \sum_{v=1}^{NV_b} P_{v,t,s}^{pv} + \sum_{es=1}^{NES_b} (PD_{es,t,s} - PC_{es,t,s}) - \sum_{e=1}^{NEB_b} EB_{e,t,s} - \sum_{el=1}^{NEL_b} EL_{el,t,s}^{dr} \tag{29}$$

$$\sum_{(b,b')\in LE} QF_{b,b',t,s} = QF_{b,b'',t,s} - x_{b,b''}(i_{b,b'',t,s})^2 + Q_{t,s}^{mt} + \sum_{i=1}^{NP_b} Q_{i,t,s} + \sum_{w=1}^{NW_b} Q_{w,t,s}^{wind} + \sum_{v=1}^{NV_b} Q_{v,t,s}^{pv} - \sum_{el=1}^{NEL_b} QL_{el,t,s}^{dr} \tag{30}$$

$$v_{b,t,s} - v_{b',t,s} = (r_{b,b'} PF_{b,b',t,s} + x_{b,b'} QF_{b,b',t,s}) - (r_{b,b'}^2 + x_{b,b'}^2) i_{b,b',t,s} \tag{31}$$

$$(v_{b,t,s} i_{b,b',t,s})^2 \ge PF_{b,b',t,s}^2 + QF_{b,b',t,s}^2 \tag{32}$$

$$v_b^{\min} \le v_{b,t,s} \le v_b^{\max} \tag{33}$$

$$0 \le i_{b,b',t,s} \le i_{b,b'}^{\max} \tag{34}$$

3.1.3 HDN's constraints

As mentioned above, the mass flow rate and temperature of the HDN are variable, leading to the use of the VF-VT control strategy in the HDN. The proposed control strategy is subject to thermal and hydraulic limitations. The relation between mass flow rate (tons/hour) and heat energy (MW) generated by GF-CHP and EB units are presented by (35) and (36). The relationship between heat generated and power consumption of the EB unit is expressed by (37) [14].

$$M_{i,t,s} = 3600\ H_{i,t,s} / c^{p}(T^{su}_{h,t,s} - T^{re}_{h,t,s}) \quad i \in NCHP \tag{35}$$

$$M^{EB}_{e,t,s} = 3600\, H^{EB}_{e,t,s} / c^{p}(T^{su}_{h,t,s} - T^{re}_{h,t,s}) \tag{36}$$

$$H^{EB}_{e,t,s} = COP_{e} EB_{e,t,s} \tag{37}$$

The limitations of the HDN-connected HSS are also defined as (38)-(42). Limitations on HSS charging and discharging power are described by (38) and (39), respectively. The hourly energy level stored in the HSS and its capacity limit are defined by (40) and (41), respectively. As shown in (42), the initial and final energy levels of HSS should be the same. The relationships between mass flow rate and heat consumed and generated by HSS are presented as (43) and (44) [14, 28].

$$0 \le HC_{hs,t,s} \le HC^{\max}_{hs} \tag{38}$$

$$0 \le HD_{hs,t,s} \le HD^{\max}_{hs} \tag{39}$$

$$HS_{hs,t,s} = HS_{hs,t\text{-}1,s} + \eta^{hs\_ch}_{hs} HC_{hs,t,s} - \frac{HD_{hs,t,s}}{\eta^{hs\_dis}_{hs}} \tag{40}$$

$$0 \le HS_{hs,t,s} \le HS^{\max}_{hs} \tag{41}$$

$$HS_{hs,t=0} = HS_{hs,t=24,s} \tag{42}$$

$$MC_{hs,t,s} = 3600\ HC_{hs,t,s} / c^{p}(T^{su}_{h,t,s} - T^{re}_{h,t,s}) \tag{43}$$

$$MD_{hs,t,s} = 3600\ HD_{hs,t,s} / c^{p}(T^{su}_{h,t,s} - T^{re}_{h,t,s}) \tag{44}$$

Constraint (45) points out that the heat demand decreased in each hour should be shifted to other hours. Heat demand after implementing IDR is denoted by (46). Shiftable heat demand in each hour is limited, as determined by (47). The relationship between mass flow rate and heat demand is expressed as (48) [28].

$$\sum_{t=1}^{NT} (HLR^{up}_{hl,t,s} - HLR^{dn}_{hl,t,s}) = 0 \tag{45}$$

$$HL_{hl,t,s}^{dr} = HL_{hl,t}^{0} + HLR_{hl,t,s}^{up} - HLR_{hl,t,s}^{dn} \tag{46}$$

$$HL_{hl,t}^{0}(1-\chi_{hl}^{H}) \le HL_{hl,t,s}^{dr} \le HL_{hl,t}^{0}(1+\chi_{hl}^{H}) \tag{47}$$

$$M_{hl,t,s}^{HL} = 3600\, H_{hl,t,s}^{dr} / c^{p}(T_{h,t,s}^{su} - T_{h,t,s}^{re}) \tag{48}$$

According to the law of conservation of energy, when liquids enter the same node at different temperatures, the mixed temperature in supply and return pipelines are calculated by (49) and (50). Additionally, the temperature of the input mass flows is equal to the temperature when mixing in the node, as described by (51) and (52) [14].

$$\begin{aligned}&\sum_{j\in AS^{-}} M_{j,t,s}^{su} T_{j,t,s}^{su,out} + \sum_{i=1}^{NCHP_h} M_{i,t,s} T_{j,t,s}^{su,out} + \sum_{e=1}^{NEB_h} M_{e,t,s}^{EB} T_{j,t,s}^{su,out} + \sum_{hs=1}^{NHS_h} MD_{hs,t,s} T_{j,t,s}^{su,out} \\ &= T_{h,t,s}^{su}\Big(\sum_{j\in AS^{-}} M_{j,t,s}^{su} + \sum_{i=1}^{NCHP_h} M_{i,t,s} + \sum_{e=1}^{NEB_h} M_{e,t,s}^{EB} + \sum_{hs=1}^{NHS_h} MD_{hs,t,s}\Big)\end{aligned} \tag{49}$$

$$\sum_{j\in AR^{-}} (M_{j,t,s}^{re} T_{j,t,s}^{re,out}) + \sum_{hl=1}^{NHL_h} M_{hl,t,s}^{HL} T_{j,t,s}^{re,out} + \sum_{hs=1}^{NHS_h} MC_{hs,t,s} T_{j,t,s}^{re,out} = T_{h,t,s}^{re}\Big(\sum_{j\in AR^{-}} M_{j,t,s}^{re} + \sum_{hl=1}^{NHL_h} M_{hl,t,s}^{HL} + \sum_{hs=1}^{NHS_h} MC_{hs,t,s}\Big) \tag{50}$$

$$T_{j,t,s}^{su,in} = T_{h,t,s}^{su} \quad \forall j \in AS^{+} \tag{51}$$

$$T_{j,t,s}^{r,in} = T_{h,t,s}^{r} \quad \forall j \in AR^{+} \tag{52}$$

The fluid temperature in the pipelines decreases with the flow direction due to the unavoidable heat loss. The relationships between each pipeline's input and output temperatures are formulated as (53) and (54). The relevant limitations of the supply and return temperatures are defined as (55) and (56) [16].

$$T_{j,t,s}^{su,out} = (T_{j,t,s}^{su,in} - T_g) e^{-\frac{L_j U_j}{c^p M_{j,t,s}^{su}}} + T_g \tag{53}$$

$$T_{j,t,s}^{re,out} = (T_{j,t,s}^{re,in} - T_g) e^{-\frac{L_j U_j}{c^p M_{j,t,s}^{re}}} + T_g \tag{54}$$

$$T_{h}^{su,\min} \le T_{h,t,s}^{su} \le T_{h}^{su,\max} \tag{55}$$

$$T_{h}^{re,\min} \le T_{h,t,s}^{re} \le T_{h}^{re,\max} \tag{56}$$

The input mass flows to each node are equal to the output mass flows from that node, as defined by (57) and (58) for supply and return pipelines. The constraints related to the capacity of the supply and return pipelines are also shown as (59)-(60)[17].

$$\sum_{j\in AS^{-}}^{NJ_h} M_{j,t,s}^{su} + \sum_{i=1}^{NCHP_h} M_{i,t,s} + \sum_{e=1}^{NEB_h} M_{e,t,s}^{EB} + \sum_{hs=1}^{NHS} (MD_{hs,t,s} - MC_{hs,t,s}) = \sum_{hl=1}^{NHL} M_{hl,t,s}^{HL} + \sum_{j\in AS^{+}}^{NJ_h} M_{j,t,s}^{su} \tag{57}$$

$$\sum_{j\in AR^{-}}^{NJ_h} M^{re}_{j,t,s} + \sum_{hl=1}^{NHL_h} M^{HL}_{hl,t,s} = \sum_{j\in AR^{+}}^{NJ_h} M^{re}_{j,t,s} + \sum_{i=1}^{NCHP_h} M_{i,t,s} + \sum_{e=1}^{NEB_h} M^{EB}_{e,t,s} + \sum_{hs=1}^{NHS} (MD_{hs,t,s} - MC_{hs,t,s}) \quad (58)$$

$$0 \le M^{su}_{j,t,s} \le M^{su,\max}_{j,t,s} \quad (59)$$

$$0 \le M^{re}_{j,t,s} \le M^{re,\max}_{j,t,s} \quad (60)$$

It is noticeable that pressure changes occur in heating network pipelines due to friction that can be considered in the proposed model. As pressure loss is made during water transfer, a water pump is needed to direct the water flow. The pump's power consumption is relevant to the mass flow rate and the pressure difference that can be included in the proposed model. However, in this paper, the power consumption of circulating pumps have not been ignored as the power consumed by these pumps is far less than EBs and cannot significantly impact the optimal dispatch of units and daily operation cost [14, 28, 35].

3.1.2 GDN's constraints

The amount of gas consumed by GF-CHP units for generating power and heat is expressed by (59) and (60). Equation (61) represents the capacity limitation of gas suppliers managed by the MEDC operator. The relevant restrictions of ramp-up and ramp-down rates of gas-suppliers in consecutive time intervals are stated by (62) and (63). Equation (64) ensures that the gas demand curtailed in each hour should be shifted to other hours. Constraint (65) shows the gas demand after applying IDR. Shiftable gas demand in each hour is limited as (66). Equation (67) states the relationship of residential gas demands and GF-CHP units with each node of the GDN. The constraints of the GDN-connected GSS are described as (68)-(72). The charging and discharging rate of the GSS are limited by (68) and (69), respectively. Equation (70) shows the hourly energy level in the GSS. Constraint (71) demonstrates the capacity limitation of the GSS. Equation (72) points out that the initial and final energy levels of the GSS should be the same. The flow of gas through the pipeline with and without the compressor is a function of the gas pressure at both ends of the pipeline, as provided by (73)-(75). Pressure limitation and the gas balance in each node are described as (76) and (77), respectively.

$$F^{G}_{i,t,s} = HR_i P_{i,t,s} + SG_{i,t,s} + SG_{i,t,s} \quad \forall i \in NCHP \quad (61)$$

$$F^{G}_{i,t,s} = HR^{h}_{i} H_{i,t,s} \quad \forall i \in NCHP \quad (62)$$

$$0 \le G^{\sup}_{g,t,s} \le G^{\sup,\max}_{g} \quad (63)$$

$$G^{\sup}_{g,t,s} - G^{\sup}_{g,t-1,s} \le RU^{\sup}_{g} \quad (64)$$

$$G_{g,t-1,s}^{\sup} - G_{g,t,s}^{\sup} \le RD_g^{\sup} \tag{65}$$

$$\sum_{t=1}^{NT} (GLR_{gl,t,s}^{up} - GLR_{gl,t,s}^{dn}) = 0 \tag{66}$$

$$GL_{gl,t,s}^{dr} = GL_{gl,t}^{0} + GLR_{gl,t,s}^{up} - GLR_{gl,t,s}^{dn} \tag{67}$$

$$GL_{gl,t}^{0}(1-\chi_{gl}^{G}) \le GL_{gl,t,s}^{dr} \le GL_{gl,t}^{0}(1+\chi_{gl}^{G}) \tag{68}$$

$$TGL_{k,t,s} = \sum_{gl=1}^{NGL_k} GL_{gl,t,s}^{dr} + \sum_{i=1}^{NCHP_k} F_{i,t,s}^{G} \tag{69}$$

$$0 \le GC_{gs,t,s} \le GC_{gs}^{\max} \tag{70}$$

$$0 \le GD_{gs,t,s} \le GD_{gs}^{\max} \tag{71}$$

$$GS_{gs,t,s} = GS_{gs,t\text{-}1,s} + \eta_{gs}^{gs\_ch} GC_{gs,t,s} - \frac{GD_{hs,t,s}}{\eta_{gs}^{gs\_dis}} \tag{72}$$

$$0 \le GS_{gs,t,s} \le GS_{gs}^{\max} \tag{73}$$

$$GS_{gs,t=0} = GS_{gs,t=24,s} \tag{74}$$

$$F_{k,f,t,s} = \kappa_{k,f} \sqrt{\left|\upsilon_{k,t,s}^2 - \upsilon_{f,t,s}^2\right|}\, \mathrm{sgn}(\upsilon_{k,t,s}, \upsilon_{f,t,s}) \tag{75}$$

$$F_{k,f,t,s} \ge \kappa_{k,f} \sqrt{\left|\upsilon_{k,t,s}^2 - \upsilon_{f,t,s}^2\right|}\, \mathrm{sgn}(\upsilon_{k,t,s}, \upsilon_{f,t,s}) \tag{76}$$

$$\mathrm{sgn}(\upsilon_{k,t}, \upsilon_{f,t}) = \begin{cases} 1 & \upsilon_{k,t} \ge \upsilon_{f,t} \\ -1 & \upsilon_{k,t} < \upsilon_{f,t} \end{cases} \tag{77}$$

$$\upsilon_k^{\min} \le \upsilon_{k,t,s} \le \upsilon_k^{\max} \tag{78}$$

$$G_{t,s}^{mt} + \sum_{g=1}^{NG_k} G_{g,t,s}^{\sup} + TGL_{k,t,s} + \sum_{gs=1}^{NGS} (GD_{gs,t,s} - GC_{gs,t,s}) = \sum_{(k,f)\in pip} F_{k,f,t,s} \tag{79}$$

3.2. Integrated energy management under the hybrid robust-stochastic approach

There are different uncertainty management approaches to deal with uncertain parameters. The principal distinction between these approaches is in line with the various techniques applied for modelling the uncertainty of input parameters. For instance, the fuzzy technique utilizes membership functions for modelling an uncertain parameter, while the stochastic approach uses PDF. The similarity between these methods is that all of them attempt to quantify the impact of input parameters on the model's outputs. The most important methods of handling uncertainty in energy systems operation include stochastic programming, fuzzy technique, interval optimization [36], information gap decision theory [37], and robust optimization [38-40]. Robust optimization is described as a high-performance

approach to dealing with uncertainties. Soyster first presented the robust optimization in 1973 [38]. This method is suitable for situations when enough data is not available. This model does not require a PDF of uncertain parameters, so it is introduced as a valuable tool for achieving optimal solutions in optimization problems with unknown parameters. The robust optimization tries to solve the optimization problem in a way that the achieved solution is robust against any action of uncertain parameters, and it is optimal for the worst-case realization of the unknown parameter [29].

In this paper, a hybrid robust-stochastic is adopted to manage uncertainties in the energy management problem of the proposed MEDC by considering the worst condition of the market price fluctuations. The flowchart of the proposed hybrid approach is depicted in Fig. 2. The risk-neutral stochastic approach is supposed to address the stochastic nature of wind power and PV units, and the RO approach is applied to manage the uncertainty of market price. In the proposed hybrid framework, the operator can simultaneously take advantage of stochastic and robust optimization approaches to manage uncertainties. In fact, the operator is able to implement both risk-neutral and risk-averse strategies at the same time concerning the nature of uncert

ainties, which increases the flexibility of the operator's decision-making. The objective function of the proposed hybrid approach is formulated as (80) by considering the constraints (6)-(79). In the proposed model, an integer parameter Γ_s is supposed to describe the level of conservatism of the MEDC operator in the decision-making process. By increasing Γ_s in the specified time interval [0:NT], the operator adopts a decision-making model to accept more risk in the face of market price fluctuations. If $\Gamma_s = 0$ indicates that market price fluctuations are not taken into account, and if $\Gamma_s = 24$ indicates that market price uncertainty is fully involved in the decision-making process.

$$\min \sum_{s=1}^{NS} p_s \left[\sum_{t=1}^{NT} \left[\begin{array}{l} \lambda_t^{e\_mt,\min} P_{t,s}^{mt} + \lambda_t^{g\_mt} G_{t,s}^{mt} + \sum_{g=1}^{NG} C_g G_{g,t,s}^{\sup} + \sum_{i=1}^{NC} \left[\lambda^{coal} HR_i P_{i,t,s} + STC_{i,t,s} + SHC_{i,t,s} \right] \\ + \sum_{i=1}^{NP} MC_i P_{i,t,s} + \sum_{el=1}^{NEL} C_{el}^{edr} \left(ELR_{el,t,s}^{up} + ELR_{el,t,s}^{dn} \right) + \sum_{hl=1}^{NHL} C_{hl}^{hdr} \left(HLR_{hl,t,s}^{up} + HLR_{hl,t,s}^{dn} \right) \\ + \sum_{gl=1}^{NGL} C_{gl}^{edr} \left(GLR_{gl,t,s}^{up} + GLR_{gl,t,s}^{dn} \right) + \max_{\{\lambda_s \le \Gamma_s\}} \sum_{t \in \lambda_s} \left(\lambda_t^{e\_mt,\max} - \lambda_t^{e\_mt,\min} \right) \left| P_{t,s}^{mt} \right| \end{array} \right] \right] \quad (80)$$

$$s.t. \ (6)-(79) \quad (81)$$

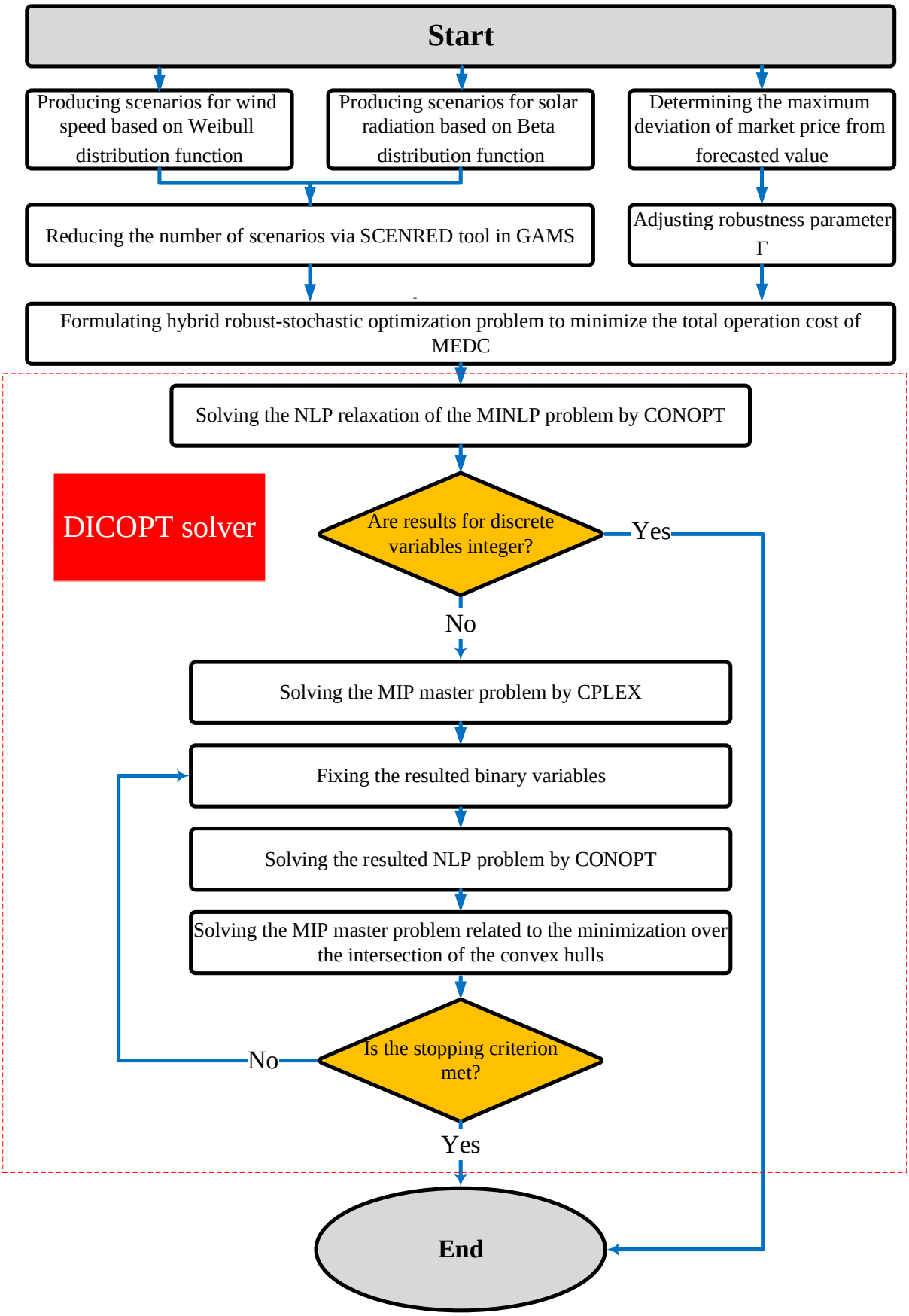

Fig. 2. Flowchart of the proposed hybrid robust-stochastic approach with DICOPT solver.

A min-max structure is made in the objective function of (80), where the outer term refers to minimizing the total operation cost of the MEDC, and the inner term models the worst condition of market price fluctuations. By updating the inner term, the objective function can be rewritten as (82) by considering the constraints (83)-(85).

$$\min \sum_{s=1}^{NS} p_s \left[\sum_{t=1}^{NT} \left[\begin{array}{l} \lambda_t^{e\_mt,\min} P_{t,s}^{mt} + \lambda_t^{g\_mt} G_{t,s}^{mt} + \sum_{g=1}^{NG} C_g G_{g,t,s}^{\sup} + \sum_{i=1}^{NC} \left[\lambda^{coal} HR_i P_{i,t,s} + STC_{i,t,s} + SHC_{i,t,s} \right] \\ + \sum_{i=1}^{NP} MC_i P_{i,t,s} + \sum_{el=1}^{NEL} C_{el}^{edr} \left(ELR_{el,t,s}^{up} + ELR_{el,t,s}^{dn} \right) + \sum_{hl=1}^{NHL} C_{hl}^{hdr} \left(HLR_{hl,t,s}^{up} + HLR_{hl,t,s}^{dn} \right) \\ + \sum_{gl=1}^{NGL} C_{gl}^{edr} \left(GLR_{gl,t,s}^{up} + GLR_{gl,t,s}^{dn} \right) + \max \sum_{t} \left(\lambda_t^{e\_mt,\max} - \lambda_t^{e\_m,\min} \right) \left| P_{t,s}^{mt} \right| z_{t,s} \end{array} \right] \right] \tag{82}$$

$$s.t.\ (4)-(77) \tag{83}$$

$$\sum_{t=1}^{NT} z_{t,s} \le \Gamma_s \ : \sigma_s \tag{84}$$

$$0 \le z_{t,s} \le 1 \ : \ \psi_{t,s} \tag{85}$$

By applying the strong duality, the proposed model in (82)-(85) can be reformulated as (86)-(92).

$$\min \sum_{s=1}^{NS} p_s \left[\sum_{t=1}^{NT} \left[\begin{array}{l} \lambda_t^{e\_mt,\min} P_{t,s}^{mt} + \lambda_t^{g\_mt} G_{t,s}^{mt} + \sum_{g=1}^{NG} C_g G_{g,t,s}^{\sup} + \sum_{i=1}^{NC} \left[\lambda^{coal} HR_i P_{i,t,s} + STC_{i,t,s} + SHC_{i,t,s} \right] \\ + \sum_{i=1}^{NP} MC_i P_{i,t,s} + \sum_{el=1}^{NEL} C_{el}^{edr} \left(ELR_{el,t,s}^{up} + ELR_{el,t,s}^{dn} \right) + \sum_{hl=1}^{NHL} C_{hl}^{hdr} \left(HLR_{hl,t,s}^{up} + HLR_{hl,t,s}^{dn} \right) \\ + \sum_{gl=1}^{NGL} C_{gl}^{edr} \left(GLR_{gl,t,s}^{up} + GLR_{gl,t,s}^{dn} \right) + \beta_{t,s} \end{array} \right] + \alpha_s \Gamma_s \right] \tag{86}$$

$$s.t.\ (4)-(77) \tag{87}$$

$$\sigma_s + \psi_{t,s} \ge \left(\lambda_t^{e\_m,\max} - \lambda_t^{e\_m,\min} \right) U_{t,s} \tag{88}$$

$$-U_{t,s} \le P_{t,s}^{e\_mt} \le U_{t,s} \tag{89}$$

$$\sigma_s \ge 0 \tag{90}$$

$$\psi_{t,s} \ge 0 \tag{91}$$

$$U_{t,s} \ge 0 \tag{92}$$

Table 2 shows the relationship between the constraints and the objective function of the proposed model, which is formulated as a mixed-integer nonlinear programming (MINLP) model and carried out in the GAMS software.

Table 2. The connection between the objective function and constraints in the proposed model

Uncertainty management approach	Stochastic approach	Hybrid robust-stochastic approach
Included uncertainties	Wind speed and solar radiation	Wind speed, solar radiation and market price
Objective function	Eq. (5)	Eq. (86)
PDN-connected resources limitations	Unit commitment for Gas-fired/non-gas-fired power plants Eqs. (6)- (15)	
	Power consumption of EB Eq. (16)	
	Power generation of wind Eq. (17)	
	Power generation of PV Eq. (18)	
	Electrical storage Eqs. (19)-(24)	
	Electricity-based demand response Eqs. (25)-(28)	
Technical limitations of PDN	Power balance Eqs. (29) and (30)	
	Relationship between voltage and current magnitudes and power flow Eq. (31)	
	Power transmission, branch current and voltage of buses Eqs. (32)-(34)	
HDN-connected resources limitations	Relationship between mass flow rate and heat generated by CHP Eqs. (35) and (36)	
	Relationship between heat generated and power consumption of EB Eq. (37)	
	Heat storage and its relationship with the mass flow rate Eqs. (38)-(44)	
	Thermal-based demand response and its relationship with the mass flow rate Eqs. (45)-(48)	
Technical limitations of HDN	Temperature balance in nodes Eqs. (49)-(51)	
	Heat losses in the pipeline Eqs. (52) and (54)	
	Nodes temperature in supply and return pipelines Eqs. (55) and (56)	
	Mass flow rate balance in nodes Eqs. (57) and (58)	
	The mass flow rate in supply and return pipelines Eqs. (59) and (60)	
GDN-connected resources limitations	Relationship between CHP units and consumed gas fuel Eqs. (61) and (62)	
	Technical limitations of gas suppliers Eqs (63)-(65)	
	Gas-based demand response Eqs. (66)-(68)	
	Gas network coupled with CHP units Eq. (69)	
	Gas storage Eqs. (70)-(74)	
Technical limitations of GDN	Gas flow in the gas pipeline with and without compressor Eqs. (75)-(77)	
	Gas pressure in gas network nodes Eq. (78)	
	Gas balance in each node Eq. (79)	
Additional constraints due to the uncertainty management approach	-	Eqs. (88)-(92)

4. Case studies and simulation results

4.1. Input data

To evaluate the suggested model, a 30-node DHN, a 20-node GDN and a 33-bus PDN are considered, as depicted in Fig. 3. The specifications of power, gas and heating distribution networks are given in [20, 35, 41], respectively. The hourly profile of power, gas and heat demands are presented in Fig. 4. The wind power plant parameters based on Eqs (1) and (2) are $P_w^{wind,max}$=1 MW, v_w^{in}=3 m/s, v_w^{out}=25 m/s, v_w^{r}=11 m/s, c=4.8 m/s and k=2 . Also, the PV system parameters based on Eqs (3) and (4) are considered as η_v^{pv}=12%, S_v^{pv}=170 m^2, α=2 and β=8. The forecasted hourly wind speed and solar irradiance are taken from [42, 43]. One thousand scenarios are generated using Monte-Carlo simulation and Eqs (1) and (3) to model uncertainties related to wind power and PV units that are reduced to ten scenarios using the SCENRED tool in GAMS software. Table 3 depicts the probability of occurrence of scenarios. The hourly power generation of wind and solar plants in each scenario are calculated by Eqs (2) and (4), respectively, which the expected hourly power of wind and solar units according to ten scenarios can be seen in Fig. 5. The forecasted electricity price is also shown in Fig. 5. The market price of natural gas is assumed to be \$2/kcf [12]. The maximum charging and discharging powers and the capacity of ESS are 1 MW, 1 MW, and 4 MWh, respectively. Likewise, the maximum charging and discharging power and the capacity of HSS are 2 MW, 2 MW and 8 MWh, respectively. The maximum rates for charging and discharging of GSS and its capacity are considered 20 kcf, 20 kcf and 100 kcf, respectively. Charging and discharging efficiencies of multi-energy storage systems are also given in [7]. The maximum supply and return temperature of the HDN is assumed to be 90 ℃ and 50 ℃, respectively. In addition, the minimum supply and return temperature of the HDN is assumed to be 70 ℃ and 30 ℃, respectively. The ambient temperature is considered to be 20 ℃. The production capacity and efficiency of the GF-CHP unit for electricity and heat generation are assumed to be 3 MW, 35% and 60%, respectively [7]. The production capacity and operating cost of the NGFPG unit are assumed to be 2 MW and \$45/MWh, respectively. The coefficient of performance of the EB unit for heat generation is also 1.2. The quantity and cost of shiftable power, heat, and residential gas demands are considered to be 10% at \$2.5/MWh, 10% at \$2.5/MWh, and 8% at \$0.4/kcf, respectively. The proposed

model is formulated as an MINLP and solved by discrete and continuous optimizer (DICOPT) powerful solver in GAMS software environment. The DICOPT can provide globally optimal outputs with a suitable degree, as used in some studies such as [28, 44, 45].

4.2. Numerical results

In the following sections, the optimal scheduling of multi-energy storage systems, power/heat generation units, gas suppliers, energy exchanged with power and gas markets and the optimal execution of IDR is analyzed by considering the physical constraints of power, gas and heat distribution networks and uncertainties related to RESs and power price.

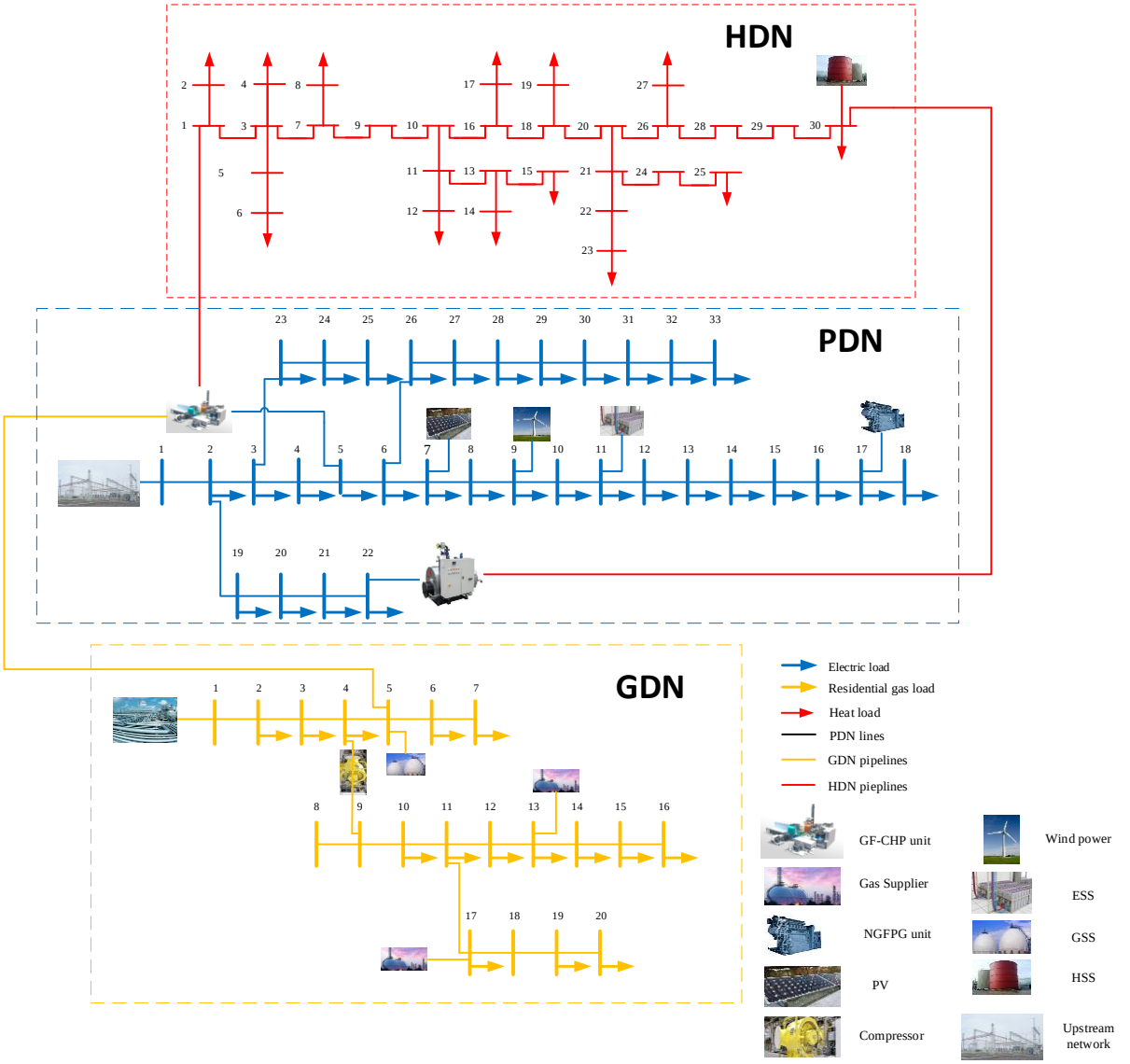

Fig. 3. The studied multi-energy distribution network

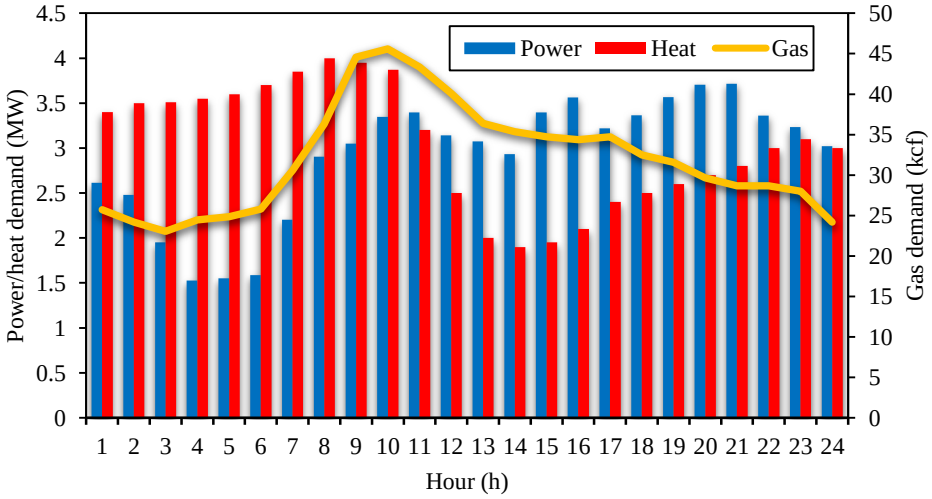

Fig. 4. The forecasted power, heat and residential gas demand

Table 3. The probability of reduced scenarios

Scenario	S1	S2	S3	S4	S5	S6	S7	S8	S9	S10
Probability	0.14	0.04	0.10	0.02	0.02	0.03	0.15	0.25	0.15	0.10

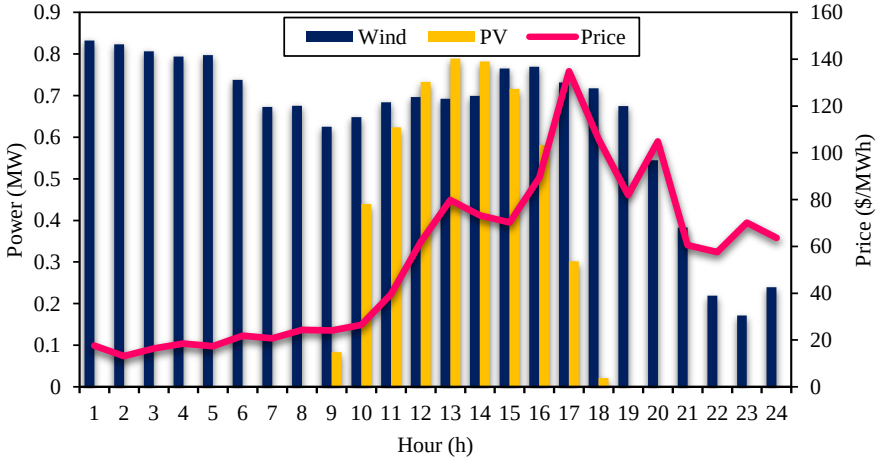

Fig. 5. The expected power generation of wind and PV units and the forecasted market price

4.2.1 Optimal scheduling of power generation resources, ESS and participation in the power market

In this section, the uncertainties associated with RESs are considered under a stochastic approach, and power price uncertainty is ignored. Figure 6 shows the expected optimal values of power generation units, ESS, power exchange with the energy market and EB's power consumption without considering IDR. The CHP unit is involved in all hours to provide part of the electrical and heat demand. However, due to GDN limitations, it is not possible to participate at full capacity during peak-price hours. The NGFPG unit undertakes to supply part of the power demand between hours 11 and 24 since the market price is higher than other hours. The ESS is operated in charge mode during hours when the power price is low (1 to 4) and then is operated in discharge mode during peak-price hours (16 to 20). The EB also

consumes a significant amount of power during off-peak price hours to generate heat. The MEDC operator prefers to participate in the power market as a buyer in the off-peak hours of power price and then participates in the market as the seller in the peak-power price hours, thus reducing the total operating cost. Under this condition, the expected operation cost is equal to $4789.44.

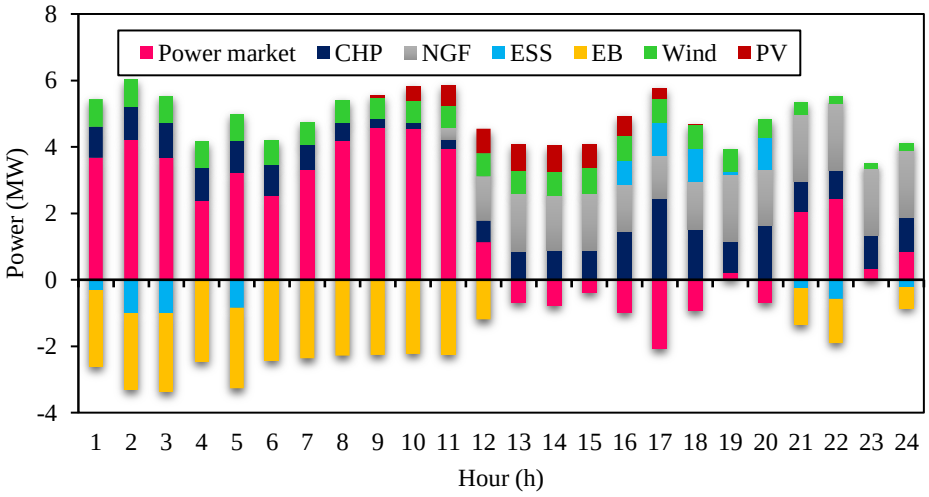

Fig. 6. The expected optimal values of generation units and energy exchanged with market

4.2.2 Optimal scheduling of heat units, gas suppliers, GSS, HSS and participation in the gas market

Figure 7 represents the expected optimal values of heat generation units and HSS. It can be seen that the CHP unit supplies a significant part of the HDN's demand. The EB unit also generates heat during off-peak power price hours. When the amount of heat generated by the CHP unit is surplus, the HSS is operated in the charging mode, and then it is switched into the discharge mode when the amount of heat generated by the CHP is low. Figure 8 demonstrates the expected optimal values of gas suppliers, the GSS and the power purchased from the gas market. The gas supply by operator-owned sources and the amount of gas purchased from the market depends on the gas distribution network constraints. Due to the limitations of the GDN, the operator buys only part of its demand from the gas market, while the rest is met by the resources under its ownership. GSS is used in charge mode between hours 1 and 11 and then is discharged between hours 13 and 20. In fact, GSS works to increase the fuel delivered to the GF-CHP unit during peak-price hours, which leads to increaseing the participation of the GF-CHP unit in the power market. Table 4 also demonstrates the effect of various energy storage systems on the entire operation cost. Excluding multi-energy storage systems, it can be seen that the operating cost is $5331.88, while in the presence of multi-energy storage systems, the operation cost is reduced to

$4789.44, which represents an 11.3% reduction in the operation cost of the MEDC. Therefore, the simultaneous consideration of multi-energy storage systems can significantly reduce the operation cost, which shows the proper performance of these technologies to serve the demand of multi-energy users.

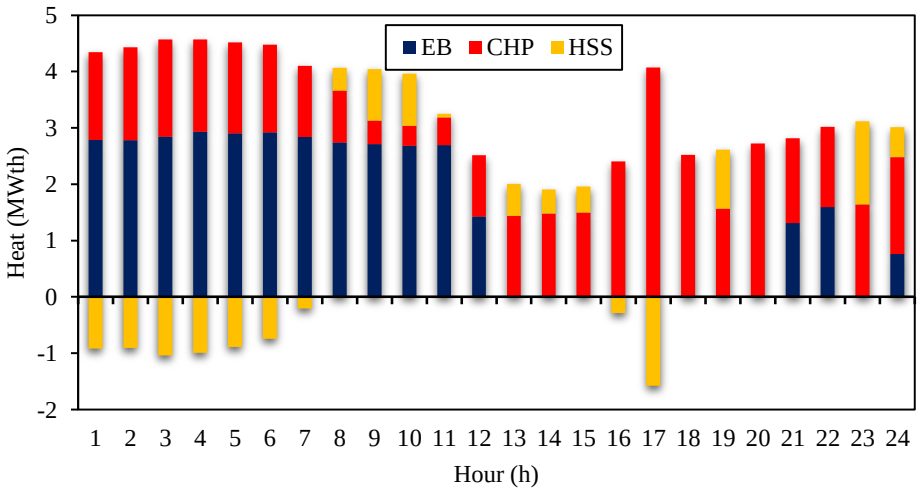

Fig. 7. The expected optimal values of heat generation units and HSS

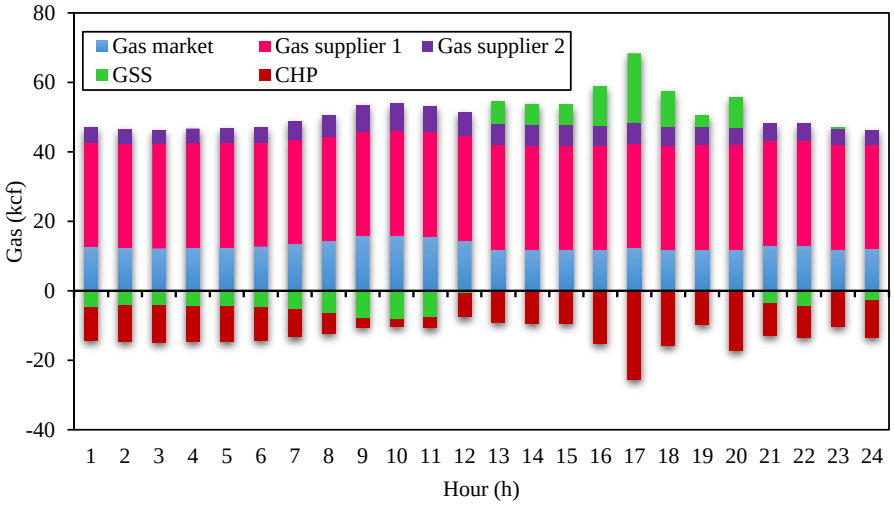

Fig. 8. The expected optimal values of gas units and gas purchased from market

Table 4 The effect of multi-energy storage systems on the total operation cost

Storages	-	ESS	GSS	HSS	Multi-energy storage systems
Total operation cost ($)	5331.88	5157.99	5074.89	5081.46	4789.44

4.2.3 Analysing constraints of multi-energy distribution network

Figure 9 illustrates the hourly voltage profiles in some buses of the PDN. It can be seen that during the hours 8 to 11 when the maximum power is purchased from the power market, the highest voltage drop is observed in the PDN, which shows the relationship between increasing demand and voltage drop.

Also, between hours 11 and 24, due to the increase in the production capacity of the PDN through the participation of the NGFPG unit, PV unit and ESS, a significant part of the demand is met by the resources owned by the MEDC operator, which will increase the PDN voltage. Figure 10 also shows the hourly pressure profiles in some nodes in the GDN. It can be seen that in node 5, the gas pressure is reduced between hours 1 and 11 when the GSS is operating in charge mode. Then, in the hours between 13 and 20 when the GSS is used in the discharge mode, the gas pressure has increased. In addition, the natural gas pressure of node 13 is higher than the pressure of other nodes, which is due to the location of the gas supplier in this node, which is injecting natural gas into this node.

Figures 11 and 12 also represents the supply and return temperatures in some nodes of the HDN. In the hours of 8 to 11, the temperature of supply pipelines has significantly decreased, and the temperature of the return pipelines has increased due to the increase in heat demand during these hours. Also, during these hours, the supply temperature in node 30 has not changed significantly, which is related to the heat output of the EB unit and HSS located in this node. Besides, in hours 16 and 17, due to the EB unit turning off and the storage system not being in discharge mode, the power supply temperature decreases and the return temperature increases. Figures 13 and 14 also represent the relationship between heat demand, the average mass flow rate in pipelines, and supply and return temperature differences. It can be seen from these figures that by increasing heat demand, the mass flow rate in pipelines enhances and the temperature difference between supply and return pipelines reduces. In addition, at some hours, such as t=17, the mass flow rate and the supply and return temperature difference follow the heat demand in a different pattern from other hours due to the operation mode and heat demand of HSS. Figures 15 and 16 analyse the effect of pipelines length and ambient temperature as two important parameters in increasing heat loss and daily operation cost. As can be seen, with the increase of the length of pipelines, the amount of heat loss and daily operating cost increase, which is due to the hot water temperature drop of pipelines when transferring from one node to another. In addition, as seen in figure 16, ambient temperatures variations can cause changes in the heat loss and daily operation cost, so that its reduction leads to an increase in heat loss and operation cost.

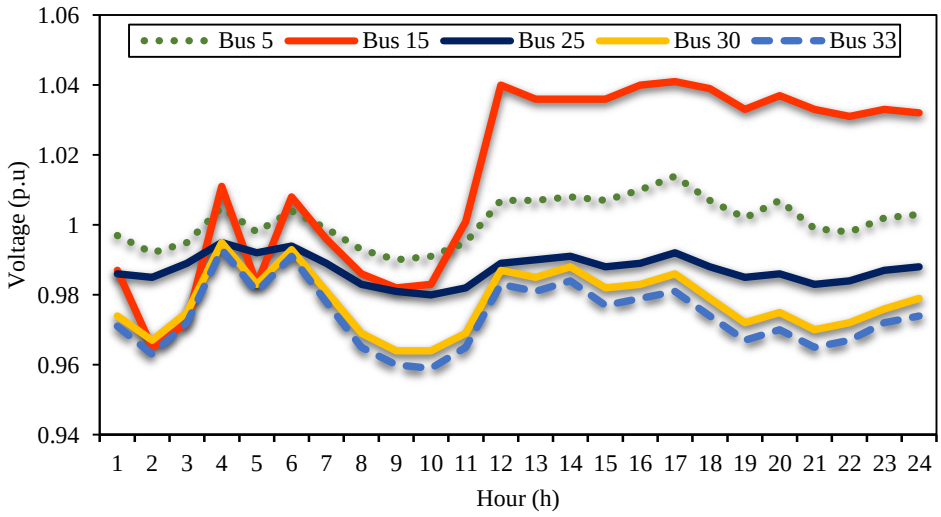

Fig. 9. The Hourly profile of buses voltage in the PDN

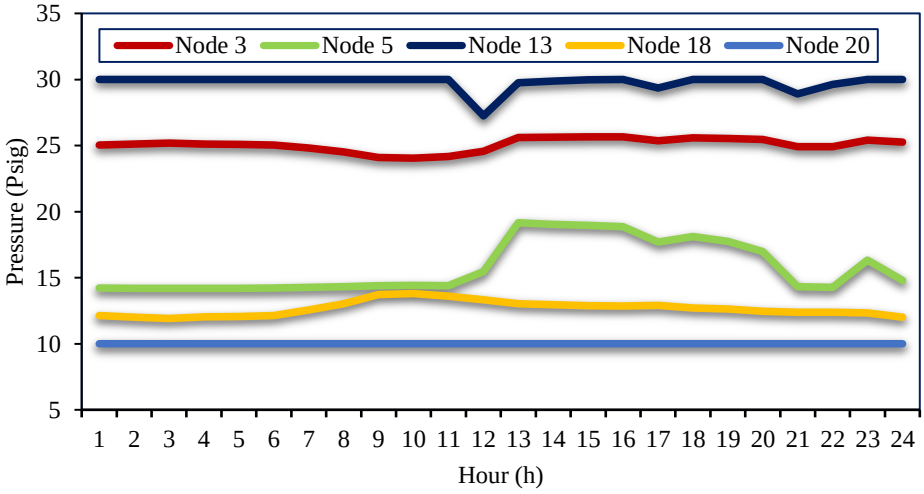

Fig. 10. The Hourly profile of nodes pressure in the GDN

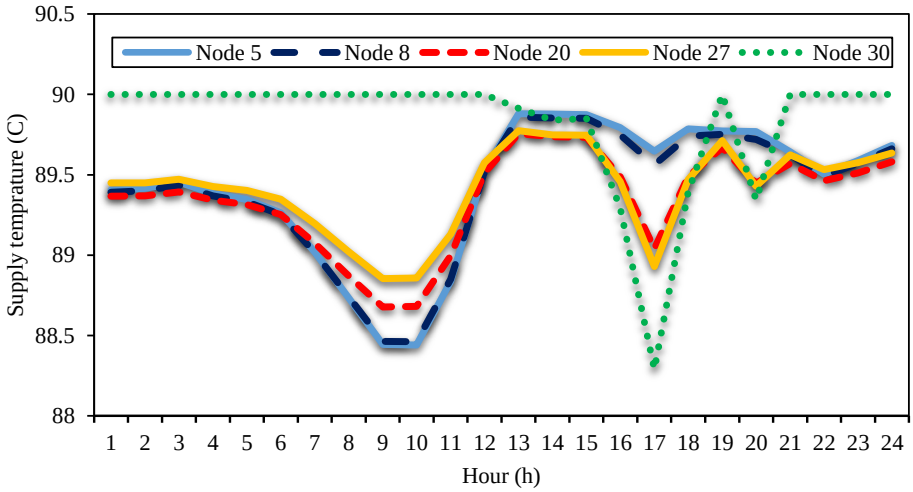

Fig. 11. The Hourly profile of supply temperature in the HDN

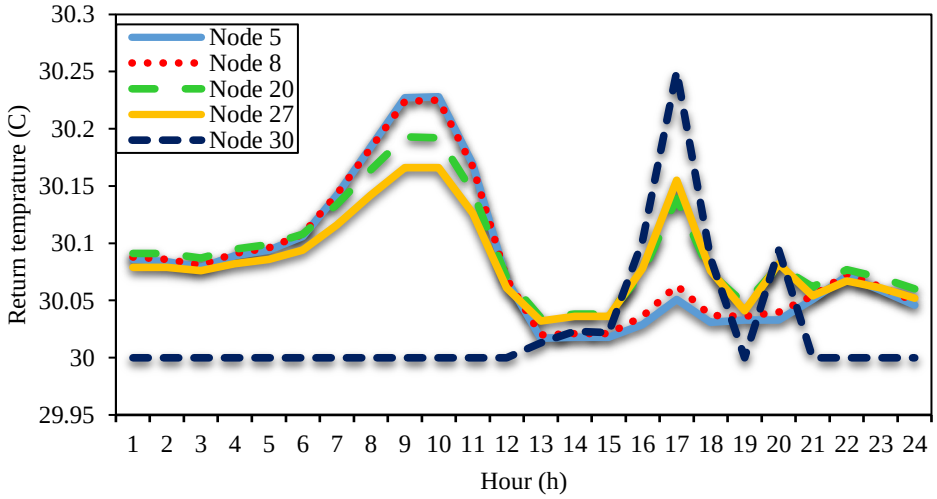

Fig. 12. The Hourly profile of return temperature in the HDN

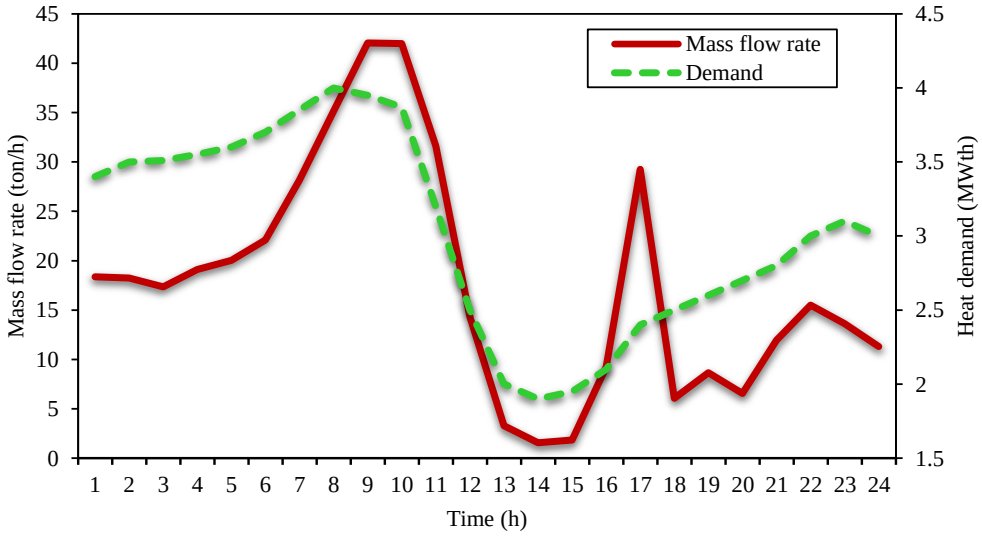

Fig. 13. The relationship between mass flow rate and heat demand

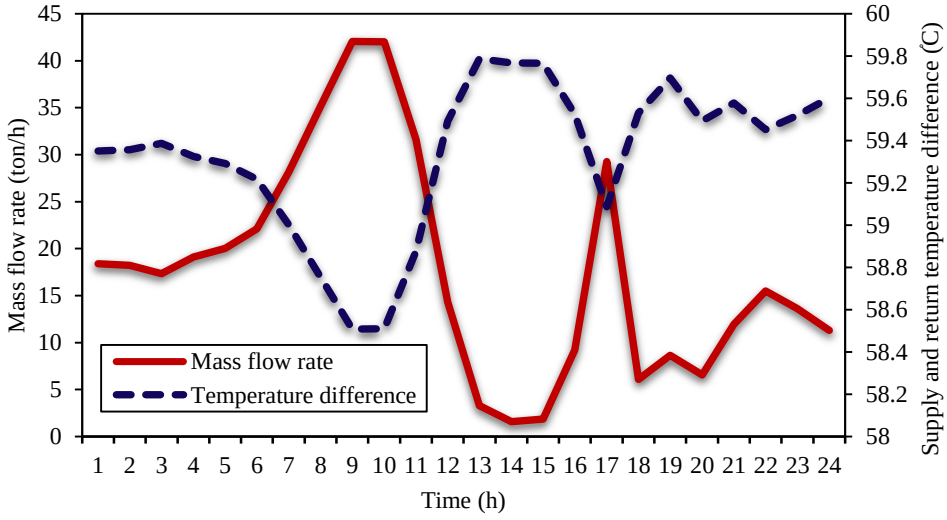

Fig. 14. The relationship between mass flow rate supply and return temperature difference

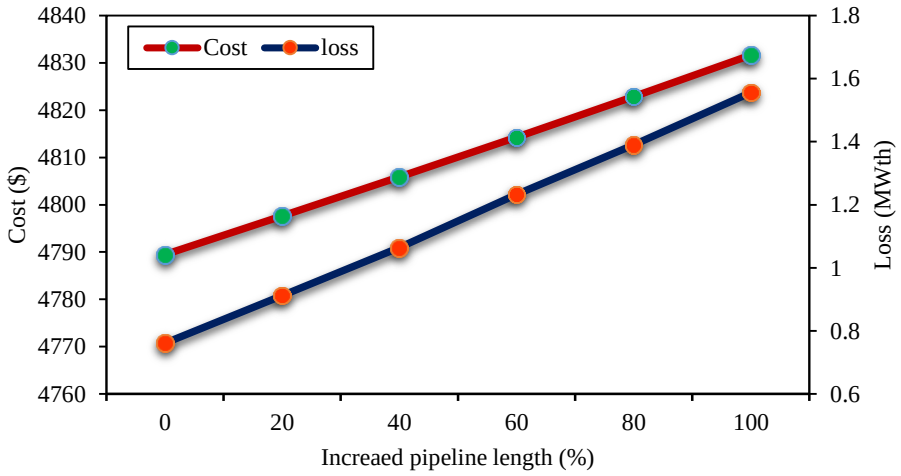

Fig. 15. The effect of pipelines length on the heat loss and daily operation cost

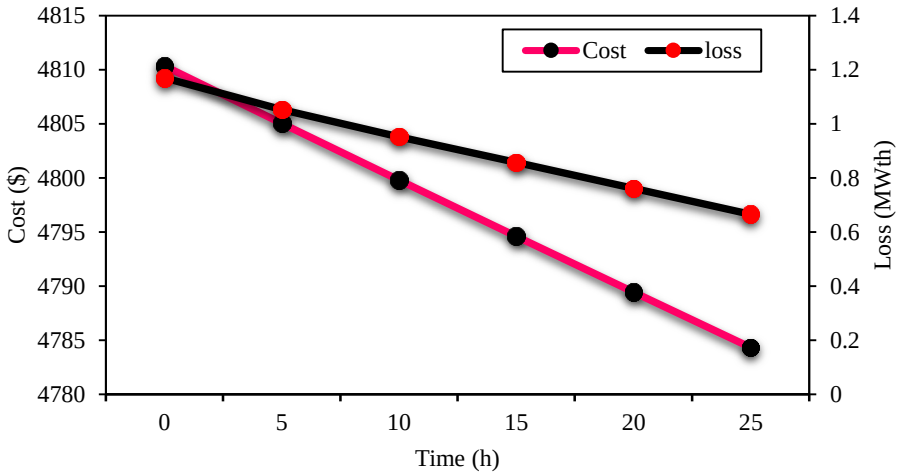

Fig. 16. The effect of ambient temperature on the heat loss and daily operation cost

4.2.3 Evaluating the impact of optimal implementation of IDR

Figure 17 depicts the effect of IDR implementation on heat and gas demand profiles. It can be seen that gas demand is decreased during the hours when the CHP unit has the most participation (between 12 and 20 hours) and is shifted to other hours. In fact, as the demand for residential gas decreases during peak price hours, the amount of gas delivered to the CHP unit increases, which leads to an increase in the GF-CHP unit's participation and the amount of power sold to the energy market during these hours. In addition, heat demand has shifted from hours when the amount of heat generated by the CHP unit is low (between 8 and 14) to other hours, which describes the dependence between the electricity distribution network and heat. The effect of IDR implementation on electricity demand and power exchanged with the energy market can be seen in Figure 18. Shifting demand from peak-price hours to

off-peak price hours leads to increasing the power sold to the energy market, which reduces the expected operation cost of the MEDC. Table 5 shows the effect of IDR implementation in the presence of multi-energy storage systems on the expected operating cost. It can be seen that in the presence of multi-energy storage systems and the optimal implementation of IDR, the operating costs have been significantly reduced compared to the conditions in which these resources are considered individually.

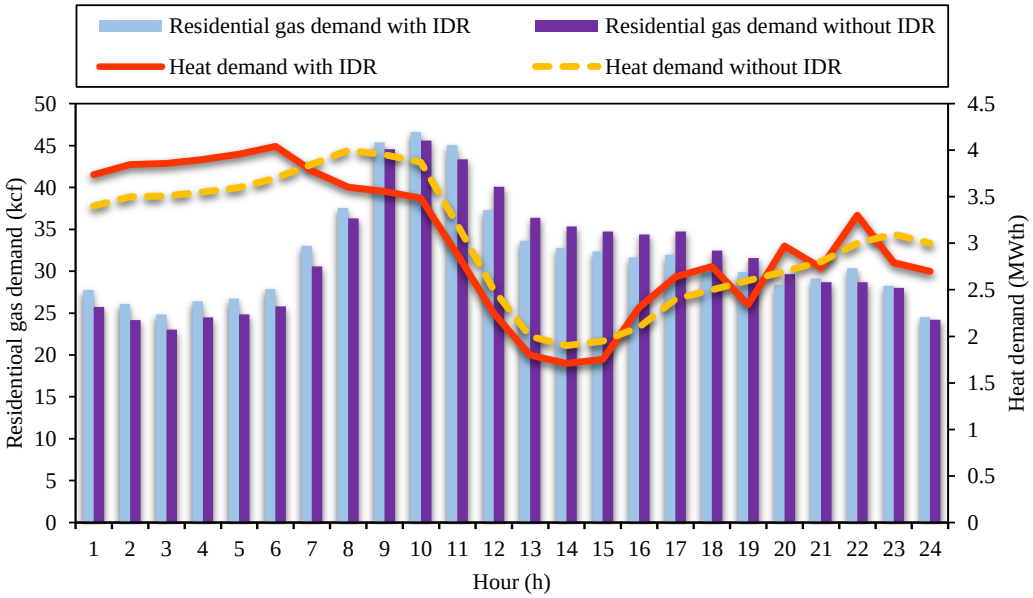

Fig. 17. The effect of IDR on the scheduled heat and gas demand

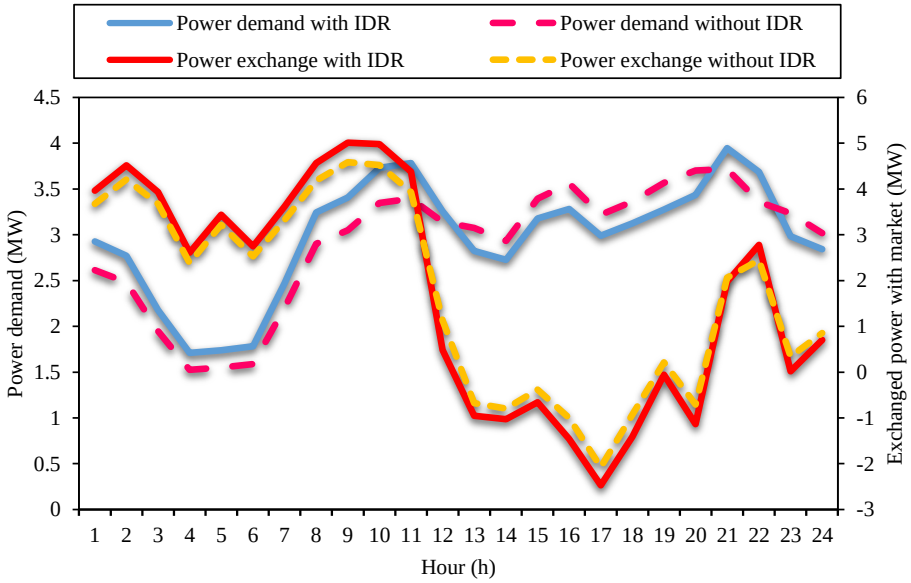

Fig. 18. The effect of IDR on the power demand and energy exchanged with market

Table 5. the effect of IDR implementation in the presence of multi-energy storage system on the operation cost

Technologies	-	IDR	Multi-energy storage	IDR and multi-energy storage system
Total operation cost ($)	5331.88	4947.86	4789.44	4578.22

4.2.4 Analysing risk-based hybrid approach

In this section, in addition to the uncertainty of RESs, market price uncertainty is also considered, which is modelled under a robust approach. The maximum deviation of the electricity price from its predicted value is assumed to be 10%. The Γ value is also considered to be 8. Figure 19 presents the effect of the robust scheduling of MEDC on the amount of power exchanged with the energy market. The amount of power purchased from the market during the off-peak price hours and the amount of power sold to the market during the peak price hours has decreased under the robust strategy, indicating that the operator prefers to reduce its power exchange with the market due to market price fluctuations. In fact, under this scheduling approach, the operator reduces its risk and applies a more conservative strategy. Figure 20 also shows the effect of robust scheduling on the power generated by the GF-CHP unit and the heat generated by the EB unit. It can be seen that under the robust approach, the heat output of the EB has reduced since it is considered as a consumer for the PDN. In contrast, the amount of power generated by the GF-CHP unit has increased significantly, meaning the operator's willingness to use the power generation resources under its ownership instead of purchasing electricity from the energy market. Figure 21 also illustrates the optimal scheduling of the multi-energy storage system. It is observed that the amount of energy stored in energy storage systems also changes by applying the robust approach, which shows the relationship between the levels of the conservatism of the MEDC with the optimal scheduling of energy storage systems. Figure 22 shows the effect of the Γ-robustness parameter on the daily operating cost. It can be seen that with increasing Γ, the total operating cost increases, which means that the MEDC operator considers a more risk-averse approach with a higher operating cost. In fact, with increasing Γ, the operator prefers to take a more conservative approach, which increases the daily operational cost.

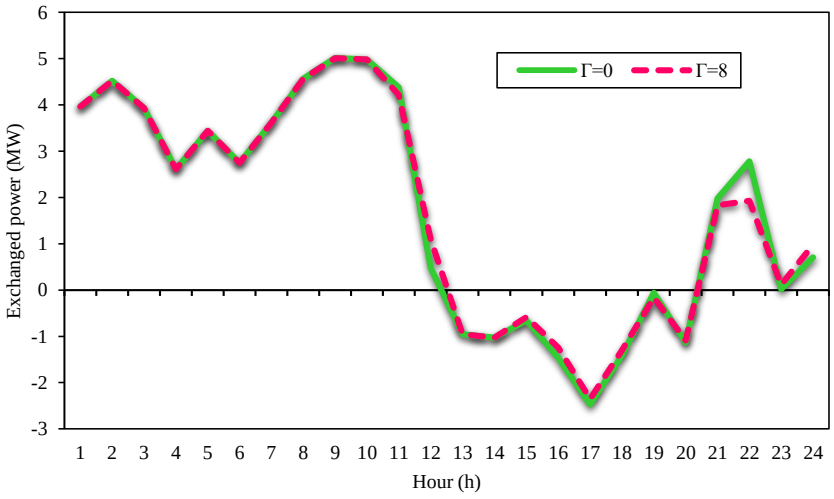

Fig. 19. The effect of risk-averse scheduling on the power exchanged with market

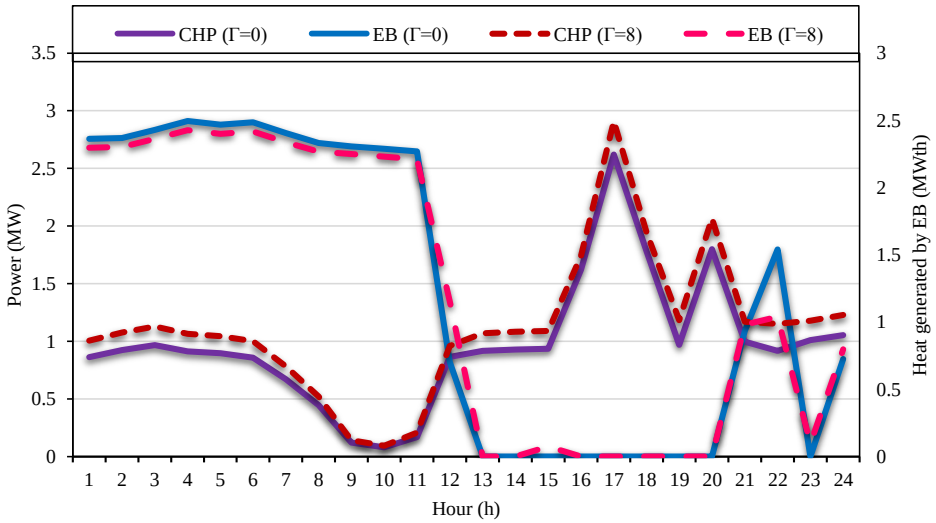

Fig. 20. The effect of risk-averse scheduling on the power dispatch of CHP and EB units

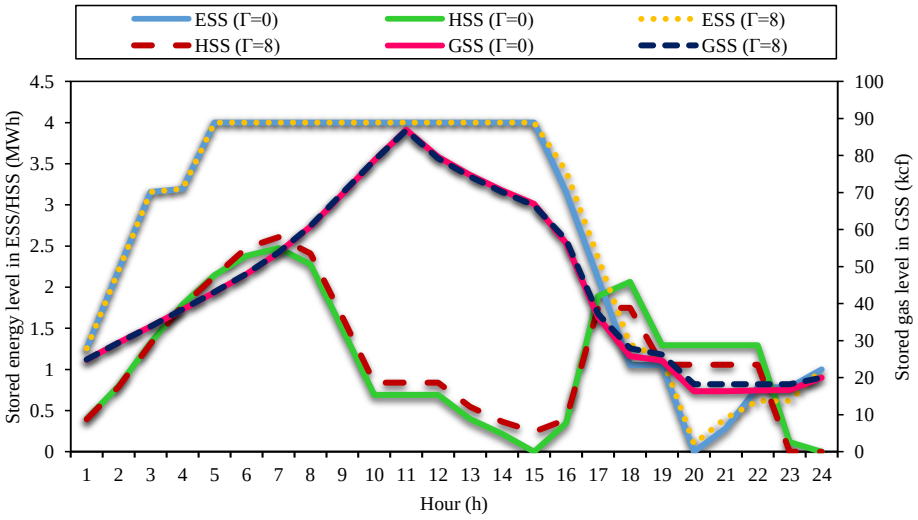

Fig 21. The effect of risk-averse scheduling on the optimal scheduling of storages

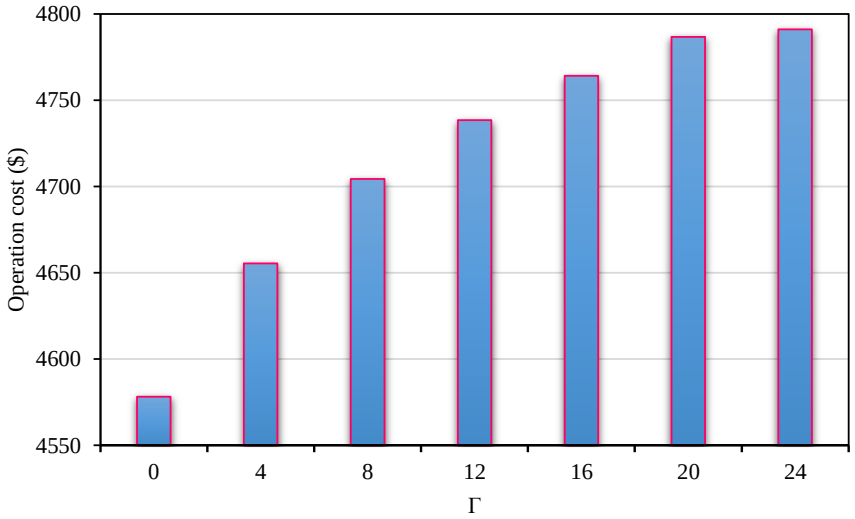

Fig. 22. The effect of the Γ-robustness parameter on the daily operating cost

5. Conclusion

This paper proposed a practical scheduling model for a new entity called multiple energy distribution company (MEDC) to supply multi-energy demand in the presence of multi-energy conversion and storage technologies. A hybrid robust-stochastic was introduced to manage uncertainties in the energy management problem of the proposed MEDC with respect to the worst-case realization of the market price fluctuations and stochastic nature of renewable energy resources. In the proposed hybrid approach, the operator was able to use both risk-neutral and risk-averse strategies at the same time due to the nature of uncertainties to adopt a more efficient decision-making model. Besides, a multi-energy flow model was introduced to model the physical constraints of the power distribution network, heating distribution network and natural gas distribution network simultaneously to achieve a practical scheduling model. A variable mass flow and variable temperature control strategy was also considered to model the heat distribution network to achieve a more efficient operation strategy. The simulation results showed an 11% reduction in total operating cost through the effective use of multiple energy storage systems to reduce the effect of multi-energy distribution network constraints on the optimal scheduling of multi-energy generation units. In addition, the optimal implementation of integrated demand response could reduce the impact of practical limitations of the multi-energy distribution network on the operation cost by 4%.

References

[1] Z. L. Hurwitz, Y. Dubief, and M. Almassalkhi, "Economic efficiency and carbon emissions in multi-energy systems with flexible buildings," *International Journal of Electrical Power & Energy Systems,* vol. 123, p. 106114, 2020.

[2] S. Haghifam, M. Dadashi, K. Zare, and H. Seyedi, "Optimal operation of smart distribution networks in the presence of demand response aggregators and microgrid owners: A multi follower Bi-Level approach," *Sustainable Cities and Society,* vol. 55, p. 102033, 2020.

[3] S. Xie, Z. Hu, J. Wang, and Y. Chen, "The optimal planning of smart multi-energy systems incorporating transportation, natural gas and active distribution networks," *Applied Energy,* vol. 269, p. 115006, 2020.

[4] P. Gao, X. Zhou, X. Yang, and Y. Li, "Sequence iterative method-based steady-state analysis of integrated electricity, gas and heating networks," *International Journal of Electrical Power & Energy Systems,* vol. 124, p. 106359, 2021.

[5] D. Mao, P. Wang, W. Wang, and L. Ni, "Reliability segment design in single-source district heating networks based on valve network models," *Sustainable Cities and Society,* vol. 63, p. 102463, 2020.

[6] J. Gu, J. Wang, C. Qi, X. Yu, and B. Sundén, "Analysis of a hybrid control scheme in the district heating system with distributed variable speed pumps," *Sustainable Cities and Society,* vol. 48, p. 101591, 2019.

[7] X. Lu, Z. Liu, L. Ma, L. Wang, K. Zhou, and N. Feng, "A robust optimization approach for optimal load dispatch of community energy hub," *Applied Energy,* vol. 259, p. 114195, 2020.

[8] P. Liu, T. Ding, Z. Zou, and Y. Yang, "Integrated demand response for a load serving entity in multi-energy market considering network constraints," *Applied Energy,* vol. 250, pp. 512-529, 2019.

[9] M. Majidi and K. Zare, "Integration of smart energy hubs in distribution networks under uncertainties and demand response concept," *IEEE Transactions on Power Systems,* vol. 34, pp. 566-574, 2018.

[10] M. Z. Oskouei, M. A. Mirzaei, B. Mohammadi-Ivatloo, M. Shafiee, M. Marzband, and A. Anvari-Moghaddam, "A hybrid robust-stochastic approach to evaluate the profit of a multi-energy retailer in tri-layer energy markets," *Energy,* vol. 214, p. 118948, 2020.

[11] E. A. M. Ceseña and P. Mancarella, "Energy systems integration in smart districts: robust optimisation of multi-energy flows in integrated electricity, heat and gas networks," *IEEE Transactions on Smart Grid,* vol. 10, pp. 1122-1131, 2018.

[12] Y. Li, Y. Zou, Y. Tan, Y. Cao, X. Liu, M. Shahidehpour, *et al.*, "Optimal stochastic operation of integrated low-carbon electric power, natural gas, and heat delivery system," *IEEE Transactions on Sustainable Energy,* vol. 9, pp. 273-283, 2017.

[13] M. A. Mirzaei, M. Z. Oskouei, B. Mohammadi-Ivatloo, A. Loni, K. Zare, M. Marzband, *et al.*, "Integrated energy hub system based on power-to-gas and compressed air energy storage technologies in the presence of multiple shiftable loads," *IET Generation, Transmission & Distribution,* vol. 14, pp. 2510-2519, 2020.

[14] Y. Cao, W. Wei, L. Wu, S. Mei, M. Shahidehpour, and Z. Li, "Decentralized operation of interdependent power distribution network and district heating network: A market-driven approach," *IEEE Transactions on Smart Grid,* vol. 10, pp. 5374-5385, 2018.

[15] J. Zheng, Z. Zhou, J. Zhao, and J. Wang, "Integrated heat and power dispatch truly utilizing thermal inertia of district heating network for wind power integration," *Applied energy,* vol. 211, pp. 865-874, 2018.

[16] Y. Zhou, M. Shahidehpour, Z. Wei, Z. Li, G. Sun, and S. Chen, "Distributionally robust co-optimization of energy and reserve for combined distribution networks of power and district heating," *IEEE Transactions on Power Systems,* vol. 35, pp. 2388-2398, 2019.
[17] Y. Zhou, M. Shahidehpour, Z. Wei, Z. Li, G. Sun, and S. Chen, "Distributionally robust unit commitment in coordinated electricity and district heating networks," *IEEE Transactions on Power Systems,* vol. 35, pp. 2155-2166, 2019.
[18] J. Li, J. Lin, Y. Song, X. Xing, and C. Fu, "Operation optimization of power to hydrogen and heat (P2HH) in ADN coordinated with the district heating network," *IEEE Transactions on Sustainable Energy,* vol. 10, pp. 1672-1683, 2018.
[19] B. Leitner, E. Widl, W. Gawlik, and R. Hofmann, "A method for technical assessment of power-to-heat use cases to couple local district heating and electrical distribution grids," *Energy,* vol. 182, pp. 729-738, 2019.
[20] S. Chen, G. Sun, Z. Wei, and D. Wang, "Dynamic pricing in electricity and natural gas distribution networks: An EPEC model," *Energy,* vol. 207, p. 118138, 2020.
[21] P. Zhao, C. Gu, Y. Xiang, X. Zhang, Y. Shen, and S. Li, "Reactive Power Optimization in Integrated Electricity and Gas Systems," *IEEE Systems Journal,* 2020.
[22] Y. Li, Z. Li, F. Wen, and M. Shahidehpour, "Privacy-preserving optimal dispatch for an integrated power distribution and natural gas system in networked energy hubs," *IEEE Transactions on Sustainable Energy,* vol. 10, pp. 2028-2038, 2018.
[23] C. He, C. Dai, L. Wu, and T. Liu, "Robust network hardening strategy for enhancing resilience of integrated electricity and natural gas distribution systems against natural disasters," *IEEE Transactions on Power Systems,* vol. 33, pp. 5787-5798, 2018.
[24] Y. Jiang, J. Xu, Y. Sun, C. Wei, J. Wang, S. Liao, *et al.*, "Coordinated operation of gas-electricity integrated distribution system with multi-CCHP and distributed renewable energy sources," *Applied Energy,* vol. 211, pp. 237-248, 2018.
[25] S. H. R. Hosseini, A. Allahham, V. Vahidinasab, S. L. Walker, and P. Taylor, "Techno-economic-environmental evaluation framework for integrated gas and electricity distribution networks considering impact of different storage configurations," *International Journal of Electrical Power & Energy Systems,* vol. 125, p. 106481, 2021.
[26] L. Yao, X. Wang, T. Ding, Y. Wang, X. Wu, and J. Liu, "Stochastic day-ahead scheduling of integrated energy distribution network with identifying redundant gas network constraints," *IEEE Transactions on Smart Grid,* vol. 10, pp. 4309-4322, 2018.
[27] A. R. Sayed, C. Wang, J. Zhao, and T. Bi, "Distribution-level robust energy management of power systems considering bidirectional interactions with gas systems," *IEEE Transactions on Smart Grid,* vol. 11, pp. 2092-2105, 2019.
[28] M. A. Mirzaei, M. Nazari-Heris, B. Mohammadi-Ivatloo, K. Zare, M. Marzband, and S. A. Pourmousavi, "Robust Flexible Unit Commitment in Network-Constrained Multicarrier Energy Systems," *IEEE Systems Journal,* 2020.
[29] A. Mansour-Saatloo, M. A. Mirzaei, B. Mohammadi-Ivatloo, and K. Zare, "A risk-averse hybrid approach for optimal participation of power-to-hydrogen technology-based multi-energy microgrid in multi-energy markets," *Sustainable Cities and Society,* vol. 63, p. 102421, 2020.
[30] D. Wang, H. Jia, K. Hou, W. Du, N. Chen, X. Wang, *et al.*, "Integrated demand response in district electricity-heating network considering double auction retail energy market based on demand-side energy stations," *Applied Energy,* vol. 248, pp. 656-678, 2019.
[31] N. Nasiri, A. S. Yazdankhah, M. A. Mirzaei, A. Loni, B. Mohammadi-Ivatloo, K. Zare, *et al.*, "A bi-level market-clearing for coordinated regional-local multi-carrier systems in presence of energy storage technologies," *Sustainable Cities and Society,* vol. 63, p. 102439, 2020.

[32] S. Lin, G. Fan, G. Jian, and M. Liu, "Stochastic economic dispatch of power system with multiple wind farms and pumped-storage hydro stations using approximate dynamic programming," *IET Renewable Power Generation,* vol. 14, pp. 2507-2516, 2020.

[33] A. Jahani, K. Zare, L. Mohammad Khanli, and H. Karimipour, "Optimized Power Trading of Reconfigurable Microgrids in Distribution Energy Market," *IEEE Access,* vol. 9, 2021.

[34] M. Hemmati, B. Mohammadi-Ivatloo, S. Ghasemzadeh, and E. Reihani, "Risk-based optimal scheduling of reconfigurable smart renewable energy based microgrids," *International Journal of Electrical Power & Energy Systems,* vol. 101, pp. 415-428, 2018.

[35] J. Li, J. Fang, Q. Zeng, and Z. Chen, "Optimal operation of the integrated electrical and heating systems to accommodate the intermittent renewable sources," *Applied Energy,* vol. 167, pp. 244-254, 2016.

[36] N. Nasiri, A. Sadeghi Yazdankhah, M. A. Mirzaei, A. Loni, B. Mohammadi-Ivatloo, K. Zare, *et al.*, "Interval optimization-based scheduling of interlinked power, gas, heat, and hydrogen systems," *IET Renewable Power Generation,* vol. 15, pp. 1214-1226, 2021.

[37] M. A. Mirzaei, M. Nazari-Heris, B. Mohammadi-Ivatloo, K. Zare, M. Marzband, M. Shafie-Khah, *et al.*, "Network-Constrained Joint Energy and Flexible Ramping Reserve Market Clearing of Power-and Heat-Based Energy Systems: A Two-Stage Hybrid IGDT–Stochastic Framework," *IEEE Systems Journal,* 2020.

[38] A. Soroudi and T. Amraee, "Decision making under uncertainty in energy systems: State of the art," *Renewable and Sustainable Energy Reviews,* vol. 28, pp. 376-384, 2013.

[39] M. A. Mirzaei, M. Hemmati, K. Zare, B. Mohammadi-Ivatloo, M. Abapour, M. Marzband, *et al.*, "Two-Stage Robust-Stochastic Electricity Market Clearing Considering Mobile Energy Storage in Rail Transportation," *IEEE Access,* vol. 8, pp. 121780-121794, 2020.

[40] M. Sadat-Mohammadi, S. Asadi, M. Habibnezhad, and H. Jebelli, "Robust scheduling of multi-chiller system with chilled-water storage under hourly electricity pricing," *Energy and Buildings,* vol. 218, p. 110058, 2020.

[41] M. Hemmati, M. Abapour, B. Mohammadi-Ivatloo, and A. Anvari-Moghaddam, "Optimal Operation of Integrated Electrical and Natural Gas Networks with a Focus on Distributed Energy Hub Systems," *Sustainability,* vol. 12, p. 8320, 2020.

[42] M. Hemmati, B. Mohammadi-Ivatloo, M. Abapour, and A. Anvari-Moghaddam, "Optimal chance-constrained scheduling of reconfigurable microgrids considering islanding operation constraints," *IEEE Systems Journal,* vol. 14, pp. 5340-5349, 2020.

[43] C. E. Murillo-Sánchez, R. D. Zimmerman, C. L. Anderson, and R. J. Thomas, "Secure planning and operations of systems with stochastic sources, energy storage, and active demand," *IEEE Transactions on Smart Grid,* vol. 4, pp. 2220-2229, 2013.

[44] M.-A. Nasr, E. Nasr-Azadani, H. Nafisi, S. H. Hosseinian, and P. Siano, "Assessing the effectiveness of weighted information gap decision theory integrated with energy management systems for isolated microgrids," *IEEE Transactions on Industrial Informatics,* vol. 16, pp. 5286-5299, 2019.

[45] M. Ahrabi, M. Abedi, H. Nafisi, M. A. Mirzaei, B. Mohammadi-Ivatloo, and M. Marzband, "Evaluating the effect of electric vehicle parking lots in transmission-constrained AC unit commitment under a hybrid IGDT-stochastic approach," *International Journal of Electrical Power & Energy Systems,* vol. 125, p. 106546, 2020.